GEM TN-92-130

Status of GEM Baselines

Michael Marx
SSC Laboratory

July 10, 1992

Abstract:

This document summarizes GEM Baseline 1 and discusses issues and options under study for Baseline 2.

The GEM (Gammas, Electrons, Muons) experiment stresses the precise measurement of gammas, electrons and muons, and, to a lesser extent, neutrinos and hadron jets. The goal is also to produce a robust detector capable of running at luminosities beyond the design luminosity of 10**33. This philosophy is based on the belief that these are the fundamental signatures for most of the standard list of physics opportunities which might be opened up by the SSC energy and luminosity: electroweak symmetry breaking; supersymmetry and other extensions of the standard model; and top and other new quarks or leptons. GEM will have moderate capabilities in tracking and hadronic calorimetry which will round out the physics program through QCD and compositeness studies.

GEM submitted a Letter of Intent to the SSC in November 1991, which described the broad architecture of the detector conceived to fulfill the above goals. Between November and March of 1992 extensive studies of performance, engineering and cost led to an iteration of this design which was formalized in the GEM Baseline 1 (4/23/92). This documented many substantial changes to the detector including a new inner tracker (silicon and pad chambers), a larger magnet and forward field shaping, mobile magnet halves and an independent central detector support, adoption of copper as the absorber of choice for the hadron calorimetry, and integration of the forward calorimeter with the ends.

The Baseline 1 Revision submitted to the PAC represents a coherent snapshot of the GEM detector. It formed the basis of all physics performance evaluations and cost studies prepared for submission to the PAC. However, the design of the GEM detector is continuously evolving as we find better and more cost effective solutions. The goals of this evolution are to improve performance in electromagnetic calorimetry and muons while maintaining high luminosity capability, and to ensure strict adherence to our policy of design-to-cost. The detector development is also strongly influenced by improved understanding of the issues of schedule, detector assembly and access. This document presents the various issues and options under study, many of which will form the basis of Baseline 2, which is expected to be frozen by early September. Baseline 2 is expected to provide the framework for the Technical Design Report.

The GEM detector consists essentially of five active systems and three passive structures. Moving concentrically outwards, the active systems consist of inner tracking, electromagnetic (EM) calorimetry, hadronic calorimetry, muon chambers, and a magnet. The passive devices consist of two forward field shapers and a central detector support structure. A cutaway perspective view of the detector is shown in Figure 1, and sections through the detector are shown in Figures 2 and 3.

The inner tracking consists of an inner silicon tracking system surrounded by layers of wire chambers utilizing interpolating pads (IPC) for precision measurement of coordinates. The tracker is shown in Figures 4 and 5. Both inner and outer trackers use stereo layers to provide the second coordinate. The tracking detector serves to identify the primary event vertex; provide identification of photons by the absence of tracks; provide track information to aid in isolating electron, muon or photon candidates; and measure momenta of electrons and muons to aid in background rejection, identification, and sign selection. The tracker performance on sign selection is shown in Figure 6. Tracker secondary goals are full reconstruction of charged tracks in an event, secondary vertex finding, and good momentum

measurement of low momentum particles. Critical factors in the design of the system include the high expected occupancy considerations which limit the performance at high luminosity, and the amount of material in the tracking volume (including chambers themselves), which will contribute to secondary interactions of particles and photon conversions, which add to confusion in an event, add background, and can cause loss of signal. Since the precision of the silicon is 10 μm and the IPC is 50 μm, a critical concern is alignment and stability of the system to take advantage of this resolution. Critical design issues being pursued include the development of radiation hard electronics, routing of services from the tracker volume, and installation and access to the tracker and the beam pipe. We expect no major revisions to the tracking system for Baseline 2.

The electromagnetic calorimetry comprises the next layer of GEM. The goal of high precision EM calorimetry is one of the primary concerns of the GEM experiment. There are currently two options under consideration — a liquid argon/krypton sampling calorimeter, and a BaF crystal total absorption calorimeter. These are shown in Figures 7, 8 and 9. Both of these devices are intended to provide a precise measurement of the energy of electrons and photons. The EM calorimeter is also used to provide directional information for photons, and for rejection of hadronic backgrounds by shower shape or size. Signals in the EM are used to form a trigger for either electrons or photons. For BaF the challenge is to reduce systematic effects to a level commensurate with the intrinsic resolution of the calorimeter. Much progress has been made in the understanding of radiation damage to BaF. For liquid argon/krypton, the challenge is to improve the resolution beyond the state of the art for the accordion plate structure, and to reduce instrumental effects produced by gaps between modules and walls. Considerable progress has been made in the designs of accordion modules for the barrel and end caps. There is a premium to reduce the level of material in front of either calorimeter. The expected performance of the two EM options in searching for Higgs decays to gamma-gamma is shown in Figure 10.

Hadronic calorimetry in GEM is situated behind the EM and also closes the forward regions. The options under study include liquid argon and scintillating fiber calorimeters, shown in Figures 11 and 12. The function of this calorimeter is to measure hadronic energy and the tails of electromagnetic showers. It is used to help in identification of electrons and photons by isolation requirements, to measure the energies of hadronic "jets," and by energy/momentum balance to deduce the passage of energetic non-interacting particles - neutrinos or new particles. Signals in the hadron calorimetry provide trigger information for electrons and photons, high energy jets, and missing energy. There are minimal requirements on depth which are needed for energy measurements, but more stringent requirements are necessary to reduce the background particles penetrating through the calorimetry to the muon system. The calorimeter should also provide energy measurements for muons traversing the calorimetry. In the forward regions there is a premium on angular coverage very close to the beam direction to avoid losing energy which could mimic a neutrino signal.

We have determined that LKr has distinct advantages in resolution and are pursuing how to implement it. Possibilities include using LKr as an upgrade in the Baseline LAr design by simply replacing the LAr with LKr in the barrel, or as a hybrid design utilizing a stand-alone LKr EM followed by a scintillating fiber hadron calorimeter as in the BaF design, shown in Figure 13. Critical issues include studies of the transition region between the EM and hadron

(for electron/pion separation, EM leakage, jet and missing Et resolution), egress of services and signals from the liquid krypton, radiation damage to the end hadron calorimeter at high η, and optimizing the forward calorimetry with regard to technology and radiation levels for the muon system. The decision on EM calorimetry (between LKr and BaF) is expected to be made this summer, which will then catalyze the decision on the hadron calorimetry behind. We are also actively studying the optimal depth of the calorimetry which trades rates in the first muon chambers for costs. The decisions on technology will also then allow finalization of the end calorimeter geometry, which strongly influences access to the tracker volume.

The muon chambers outside the central hadron calorimetry cover down to almost 9 degrees from either beam. The muon system layout shown in Figure 14 has been optimized to meet the GEM goals of 5% momentum resolution for 500 GeV/c Pt muons at $\eta = 0$, and 13% at $\eta = 2.5$. The expected resolution is shown in Figure 15. The primary chamber functions are to provide a precise measurement of a muon trajectory, to provide a trigger signal for single and multiple muons, and to provide the correlation of a muon with the correct bunch crossing. Multiple layers of chambers form 3 superlayers, and are distributed at the beginning, middle and end of the magnetic volume to permit sagitta measurements. Options under consideration are cathode strip readout chambers for the forward regions which provide spatial and trigger information; limited streamer tubes or pressurized drift tubes in the central region, used in conjunction with resistive plate counters which provide timing, trigger, and z coordinate. Details of these technologies are shown in Figures 16-19. Critical areas in the muon system include achieving needed precision of the chambers, alignment and stability at the level of 25 μm; minimization of gaps in the coverage while minimizing the impact of support structure and material in the chambers themselves. This system should be sufficiently robust to operate at the highest SSC luminosities and at the highest muon energies likely to be encountered. This puts requirements on pattern recognition of muon tracks, and double hit resolution, to find muons near hadronic debris, or debris from electromagnetic showers induced by high energy muons themselves.

A proposal to utilize the cathode strip chambers in the barrel region is being explored. These chambers hold the promise of simplifying the overall system by utilizing uniform technology over the full solid angle, providing both bend- and non-bend-coordinates plus timing and trigger information. The chambers are an order of magnitude lighter than the drift technologies under study, and their construction allows direct survey of the precision sensing elements. The success of these chambers depends on finding low cost solutions for the large precision cathode boards and for the million plus electronics channels required in this option. The choice of technology will be made after comparative performance tests to be done at the SSC in the summer of 1992 in a cosmic ray test (TTR).

The tradeoff between acceptance and resolution deterioration and alignment complexities of overlapped chambers is being studied. An option under study is to replace the independent module support system, with integrated supports for each barrel and each end system. This system, illustrated in Figure 20, is made feasible by the large facilities and shafts required for the magnet. Advantages of such an approach include the possibility of pre-alignment and commissioning of each of the sections, reducing installation time requirements in the underground hall. Comparative studies of supporting the end muon system from either the forward field shapers or the magnet and barrel chamber system are in progress. Alignment

systems under consideration include stretched wires, lens-LED systems, lasers, and X-ray calibrations. The background radiation at the muon chambers (including soft photons, electrons, and neutrons) as a function of chamber position, low Z absorbers, and drift space is being studied, particularly in the forward direction. These studies will provide requirements for pattern recognition, which will determine the minimum number of chamber layers.

The final active GEM system is the superconducting solenoid magnet within which all other detectors sit. This magnet provides an axially symmetric field, which bends the tracks of charged particles to facilitate measurement of their momentum. Measurement of momentum occurs in the inner tracking volume and muon system volume. The magnet is in two halves, one of which is shown in Figure 21, and are independently mobile to allow access to the interior and to facilitate detector installation. The magnet is on the critical path for completion of GEM, since it needs to be installed prior to all other systems. The technical design report for the magnet is complete, an acquisition plan has been submitted, and a draft RFP has been distributed to interested vendors. It is expected that the RFP will be issued this summer, and a prime contractor will begin work with the GEM magnet team at the beginning of 1993. This schedule is not precluded by decisions in other systems, since we are in the process of defining the interfaces of all systems with the magnet, which will then permit independent evolution of these systems. Thus, for example, once the support points of the muon system on the magnet are fixed, the magnet and muon designs can proceed independently.

The forward field shapers are large cones of permeable steel, which provide a field component normal to the trajectories of forward-going muons. The field produced by this system, shown in Figure 22, must be well understood and known to high precision, both in magnitude and direction. The magnetic field is returned through air, resulting in a large volume over which its effects can be felt — in the hall and on the surface. Care must be exercised to account for this return field in other experimental components. The large field shaper mass must be supported outside of the magnet, and the magnetic forces induced must be supported by the magnet itself. Uniformity of the shaper steel is important to have good understanding of the field in the muon volume, as is the placement of permeable support structures (for the magnet, field shapers and central detector) outside the coil.

The final system is the central detector support structure which supports the calorimetry and inner tracking. This device must be self supporting and permit loading and access to the supported components, with the assistance of external structures. It is designed to occupy minimal space both radially and along the beam line, so as to minimize loss of measurement of muon tracks. Studies now indicate the viability of eliminating support gussets penetrating the muon system. Another possibility is the replacement of the continuous membrane with a pedestal which would provide greater access to the interior of the detector. In either case shown in Figure 23 the support is designed to be independent of the magnet, allowing the magnet and calorimeter/tracking systems to be independently aligned.

GEM has an electronics system which shapes and digitizes the detector outputs, and forms three levels of triggers which reduce the data flow from 60 MHz to 10 Hz. We are currently studying modifications to this architecture which would include a "virtual" Level 2, where the Level 2 algorithms are implemented in the Level 3 processors. This obviates the need for special processors, but requires 100KHz event building. For the calorimetry readout

pipeline we are still comparing an all digital approach to analog switched capacitor arrays. The output from the electronics system is recorded by the data acquisition system.

GEM also includes facilities for major fabrication, final assembly and staging of installation into the underground hall. These facilities, currently in Title 1, are shown in Figures 24 and 25. A primary driver in the design of these facilities is to maintain schedule requirements and flexibility, while reducing cost. The current design calls for shaft covers rather than headhouses because of budgetary constraints. Several cost savings features may be implemented in the surface facilities to recover the headhouses, including the merging of several facilities. An underground electronics shaft, shown in Figure 26, provides a radiation and magnetically shielded environment close enough to the detector to allow trigger processing of the fast calorimeter signals. The cryogenic storage system will be moved from its position on the floor of the underground hall to the utilities shaft providing more protection and more useful hall space. We have also initiated a study to move the low-beta quads further from the detector, which may result in more flexibility for installation and access at minimal loss of luminosity.

Considerable effort has been expended to study issues of assembly and access. Several of the key assembly steps are shown in Figures 27 - 31. The current GEM access philosophy, which impinges strongly on the detector design, assumes that short accesses will only permit maintenance of components outside the magnet, which includes much of the calorimeter and muon electronics. There is limited access shown in Figure 32 through the ends of the magnet to the muon volume, to the periphery of the end calorimetry, and to the vacuum pumps behind the forward calorimeters. During longer shut-downs the detector may be opened by a few meters, or completely opened for access to the central tracker as shown in Figures 33 and 34.

The technology and design choices for Baseline 2 will be made with broad input from measurements of prototypes, simulation and engineering studies, and full consideration of who will actually build the various systems. It will also incorporate much deeper understanding of the cost and schedule issues, including the availability of funding for the full detector or, if needed, plans for staging. We fully expect Baseline 2 to be a much improved overall experiment at a reduced cost.

FIGURE	CAPTIONS
Figure 1	Cutaway perspective view of the GEM detector
Figure 2	Quarter section of the GEM detector showing key dimensions and systems
Figure 3	Section of the GEM detector
Figure 4	Section through the GEM tracker showing key dimensions and components
Figure 5	Two axial sections through the GEM tracker
Figure 6	95% Confidence level for charge separation by GEM tracker
Figure 7	Barium Fluoride EM calorimeter
Figure 8	Liquid argon EM barrel accordion module
Figure 9	Liquid argon EM end cap accordion module
Figure 10	Performance of BaF and liquid argon EM calorimeters for Higgs decay to 2 gammas. Plots on left show expected results for BaF before and after background subtraction for various mass Higgs; those on right are similar for liquid argon.
Figure 11	Quarter section of integrated liquid argon EM, hadronic and forward calorimeter
Figure 12	Quarter section of BaF with scintillating fiber hadron and forward calorimeter
Figure 13	Hybrid liquid argon EM with scintillating fiber hadron and forward calorimeter
Figure 14	Quarter section of muon system layout
Figure 15	Pt resolution vs eta for muon system
Figure 16	Cathode strip chamber construction
Figure 17	Limited streamer drift tube construction
Figure 18	Pressurized drift tube construction
Figure 19	Resistive plate counter construction
Figure 20	Cutaway schematic of integrated support for full muon barrel during assembly
Figure 21	Perspective view of one magnet half coil
Figure 22	Contours of constant flux for one quadrant of GEM magnet
Figure 23	Finite element grids for models of central detector support utilizing membrane (left) or pedestal (right)
Figure 24	Perspective view of GEM surface facilities

FIGURE	CAPTIONS (continued)
Figure 25	Cutaway perspective of GEM underground hall
Figure 26	Section through electronics shaft
Figure 27	Assembly sequence showing first magnet half installation
Figure 28	Assembly sequence showing completion of magnet
Figure 29	Assembly sequence showing calorimeter and barrel muon chamber installation
Figure 30	Assembly sequence showing end muon chamber installation
Figure 31	Assembly sequence showing tracker installation
Figure 32	Access paths with magnet closed or partially open
Figure 33	Access to tracker with magnet halves fully open
Figure 34	Access for vacuum pipe installation

GEM DETECTOR

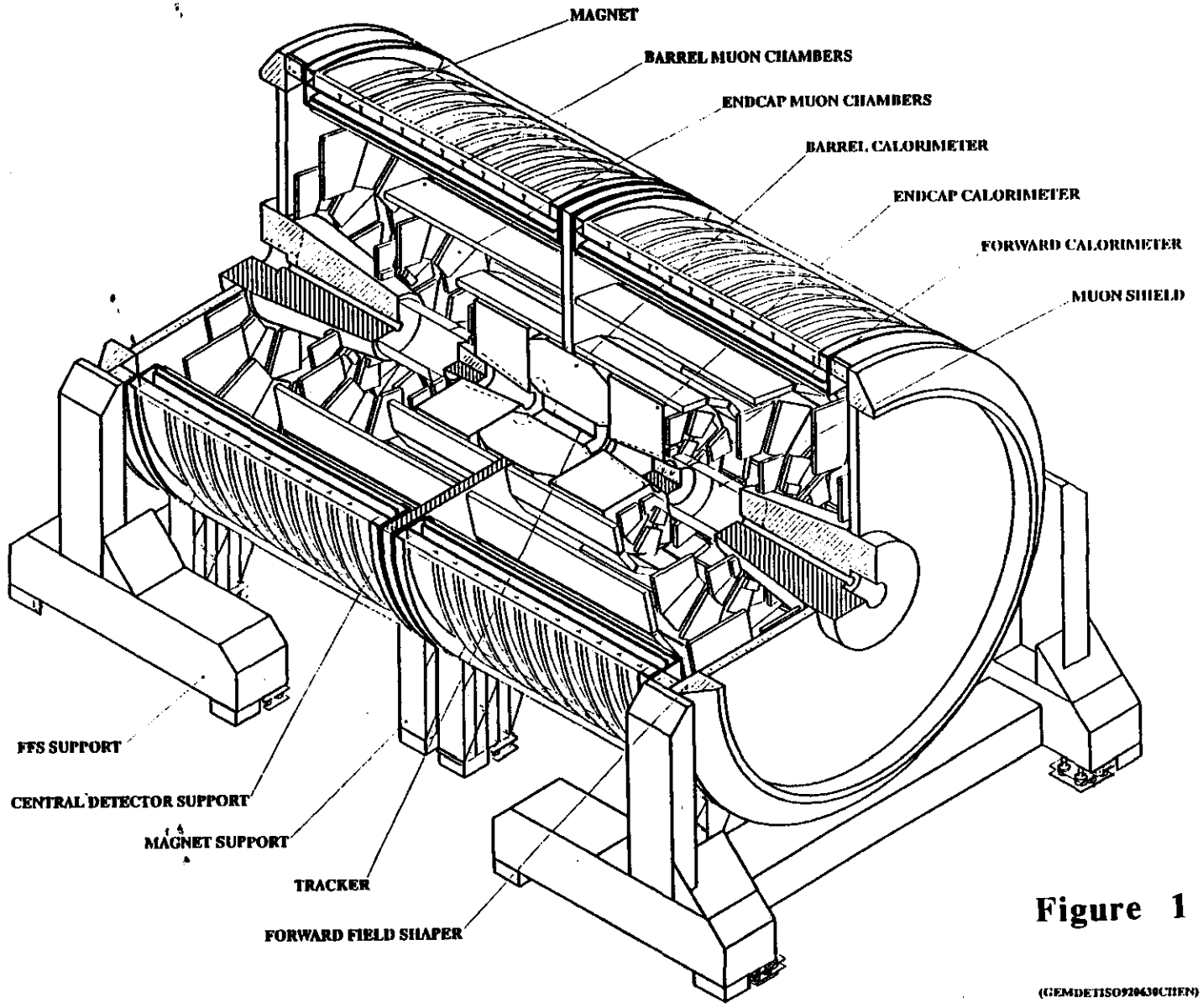

Figure 1

(GEMDETISO920630CHEN)

GEM DETECTOR ELEVATION

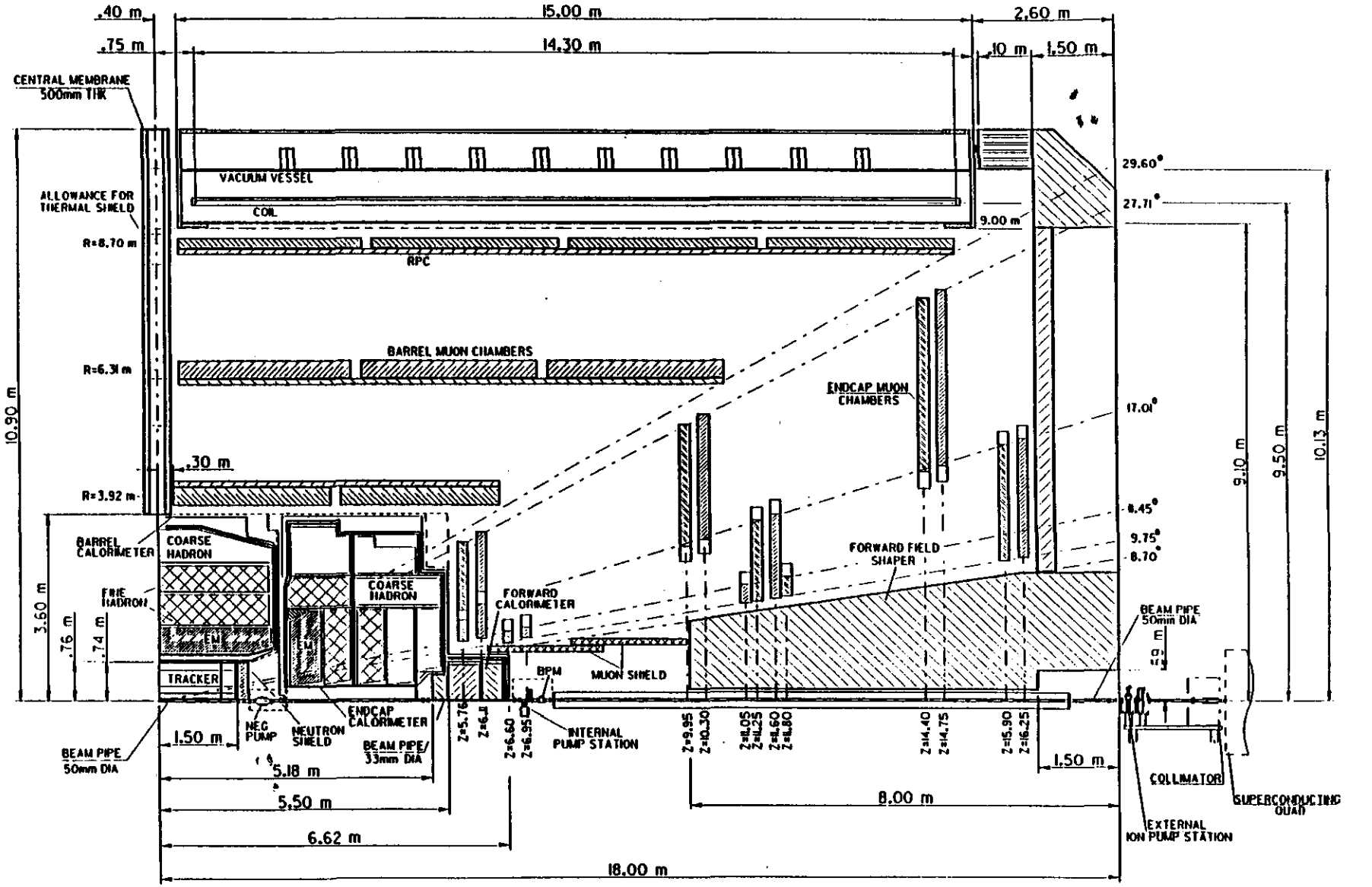

Figure 2

GEM DETECTOR LAYOUT

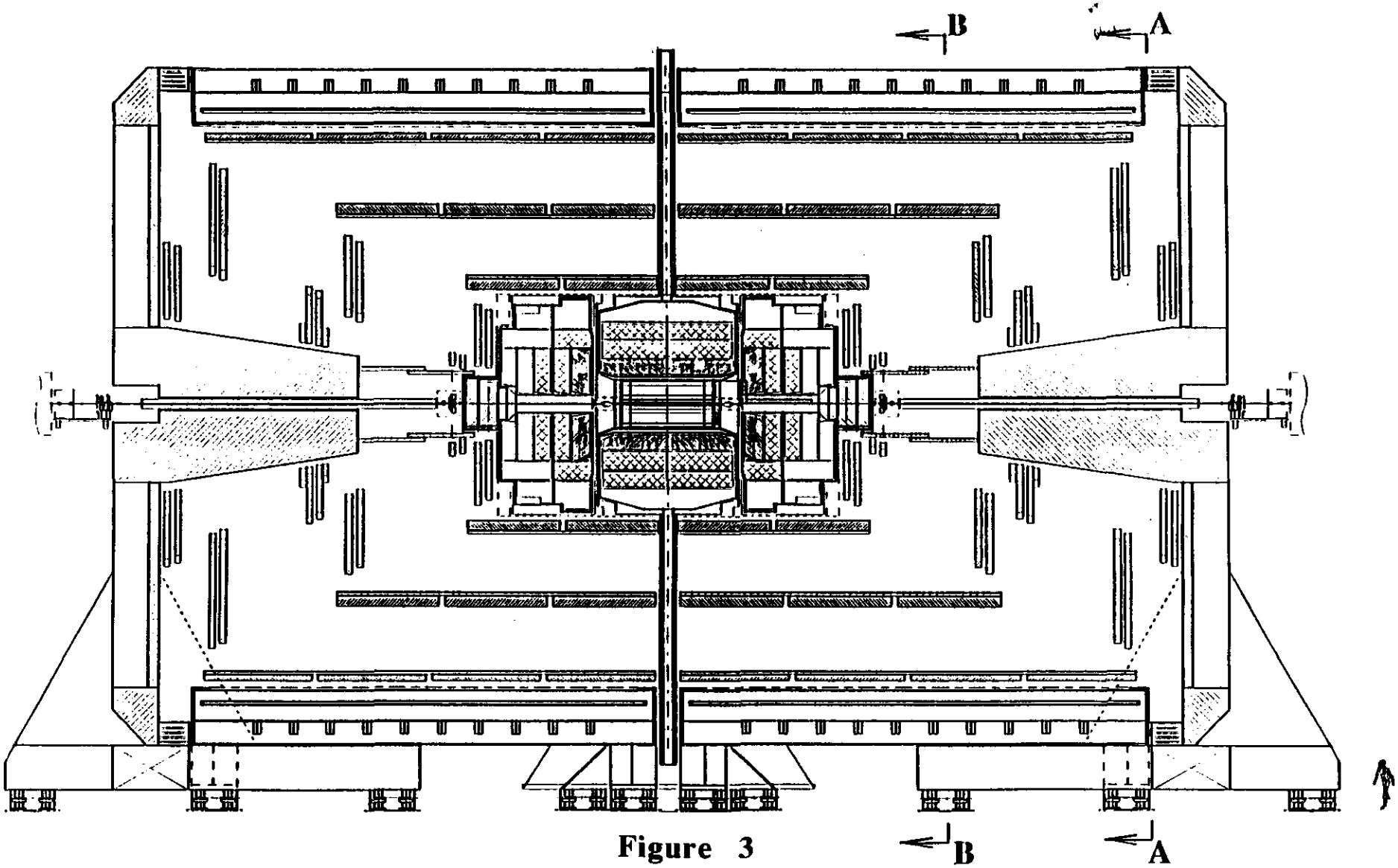

Figure 3

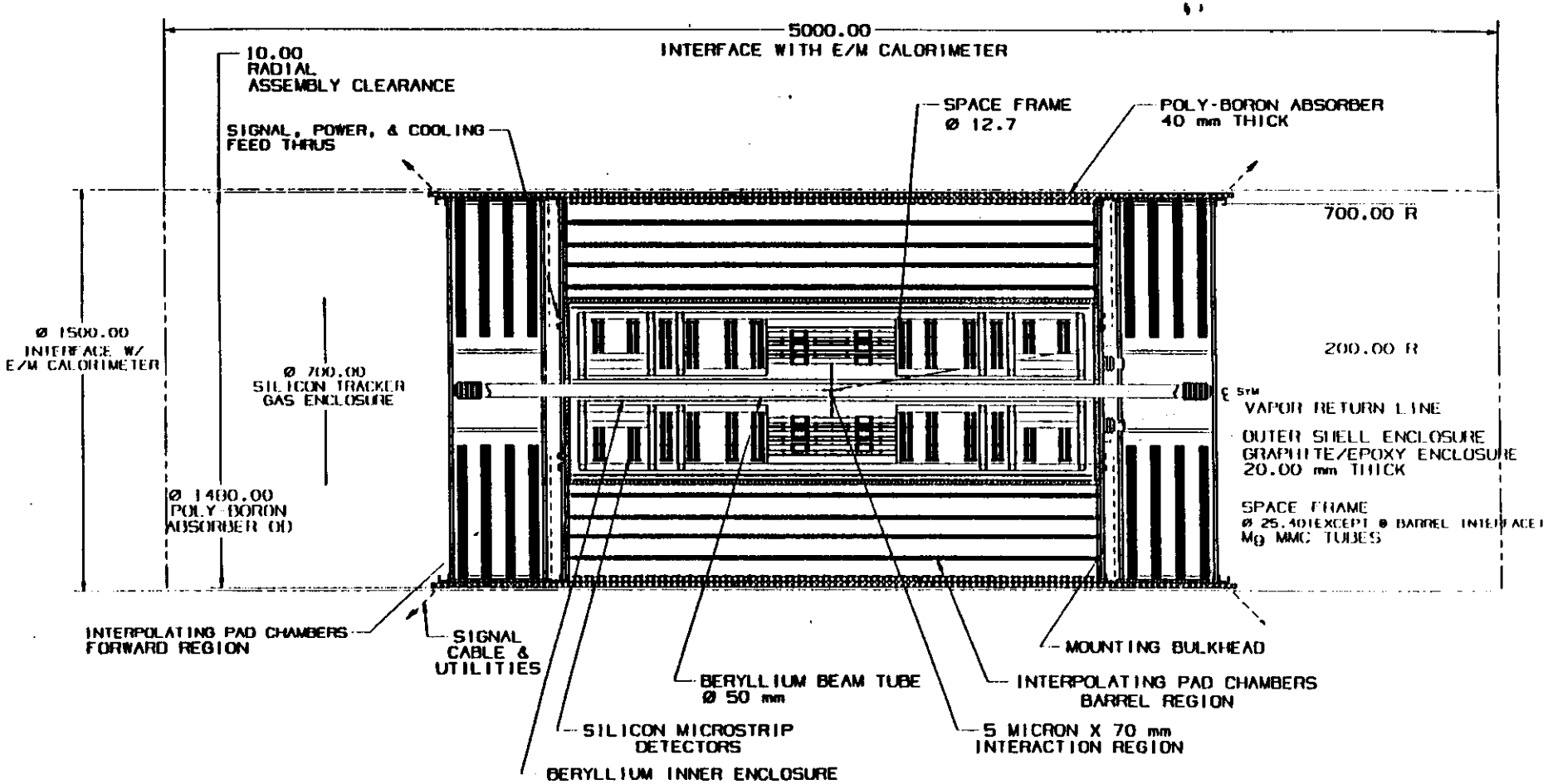

GEM CENTRAL TRACKER

Figure 4

GEMVG-126-JV

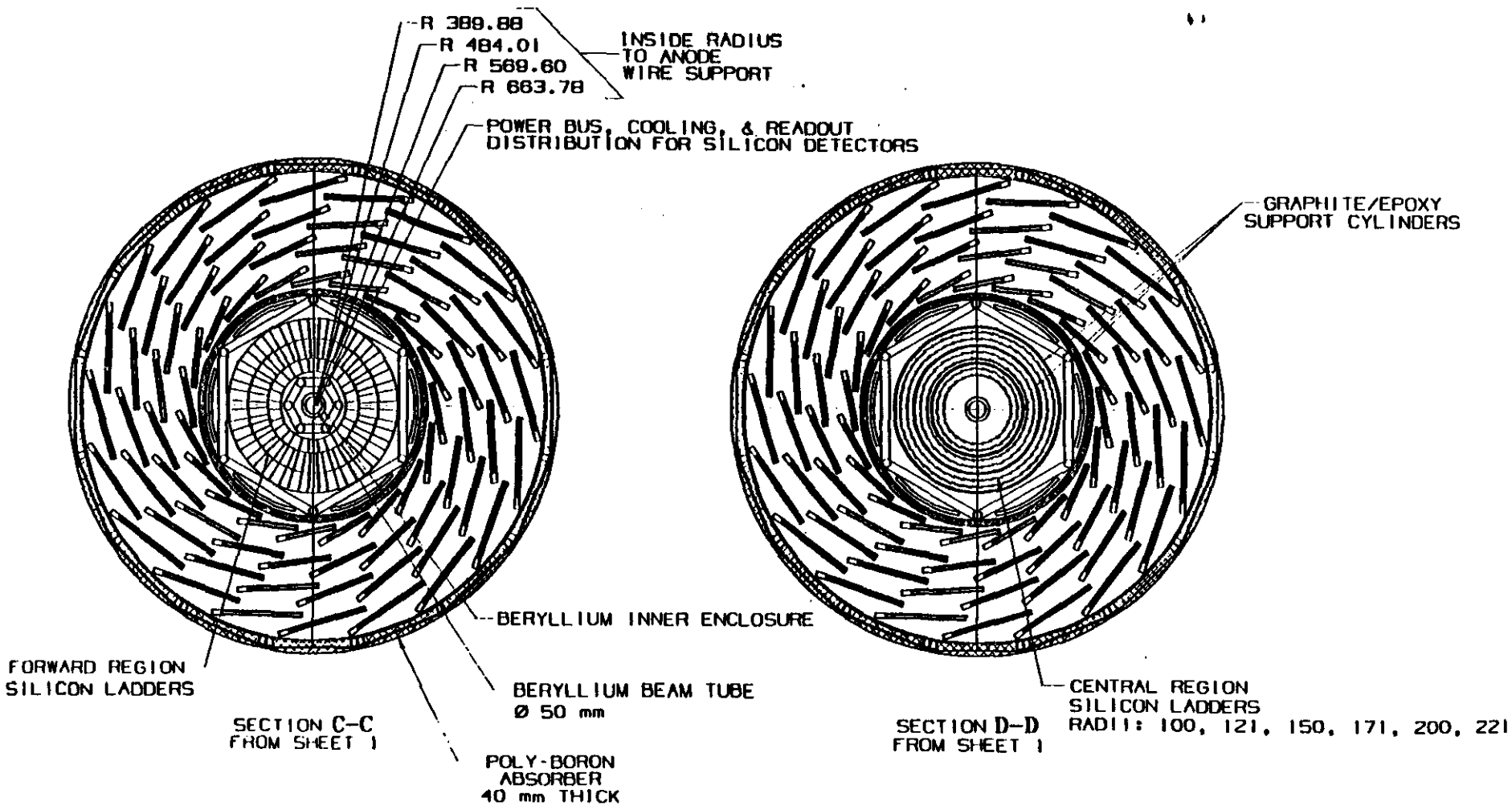
R 389.88
R 484.01
R 569.60
R 663.78
INSIDE RADIUS
TO ANODE
WIRE SUPPORT
POWER BUS, COOLING, & READOUT
DISTRIBUTION FOR SILICON DETECTORS
GRAPHITE/EPOXY
SUPPORT CYLINDERS
BERYLLIUM INNER ENCLOSURE
FORWARD REGION
SILICON LADDERS
BERYLLIUM BEAM TUBE
Ø 50 mm
SECTION C-C
FROM SHEET 1
POLY-BORON
ABSORBER
40 mm THICK
CENTRAL REGION
SILICON LADDERS
RADII: 100, 121, 150, 171, 200, 221
SECTION D-D
FROM SHEET 1

Figure 5

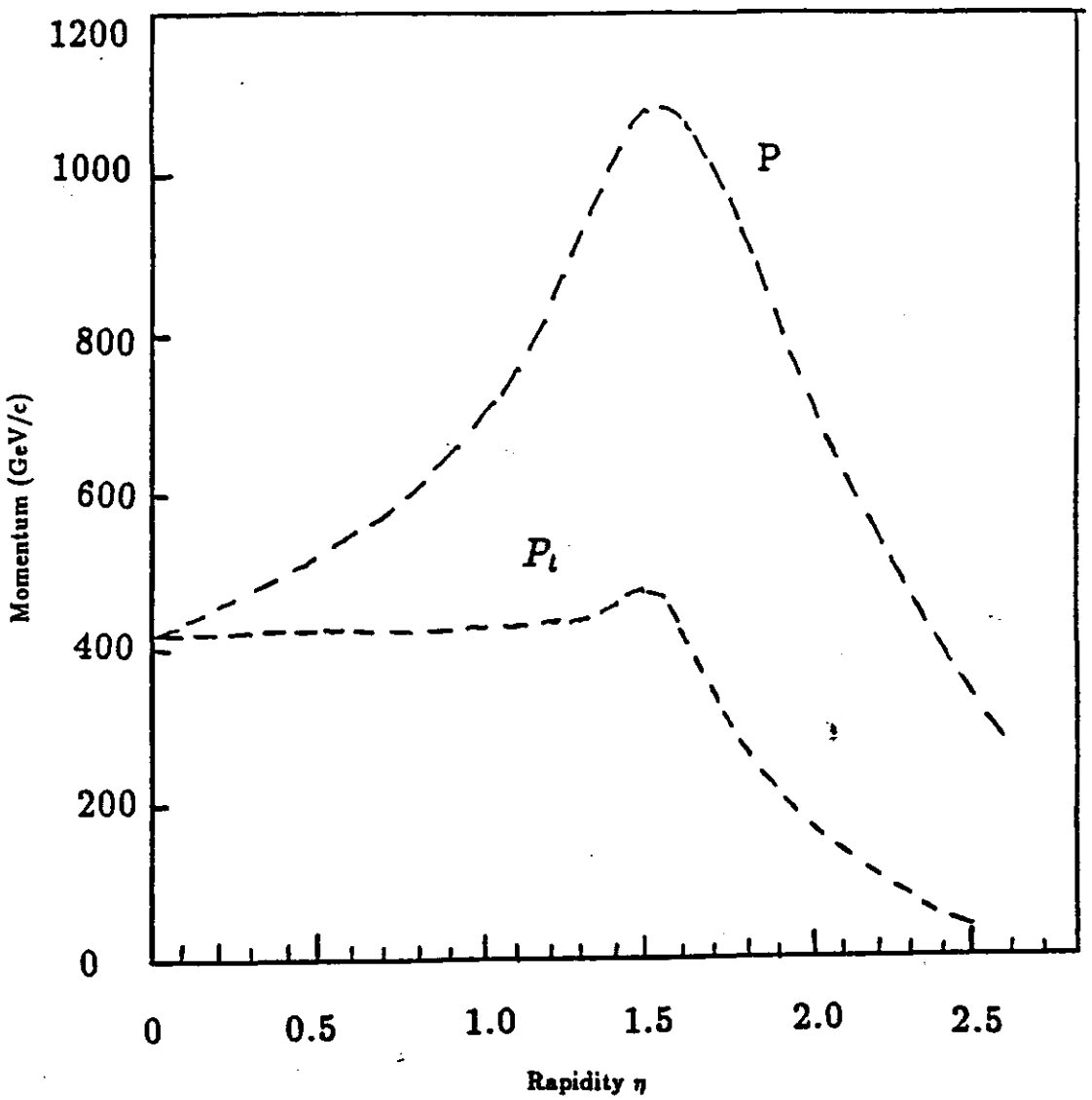

95% Confidence Level
Charge Separation

Figure 6

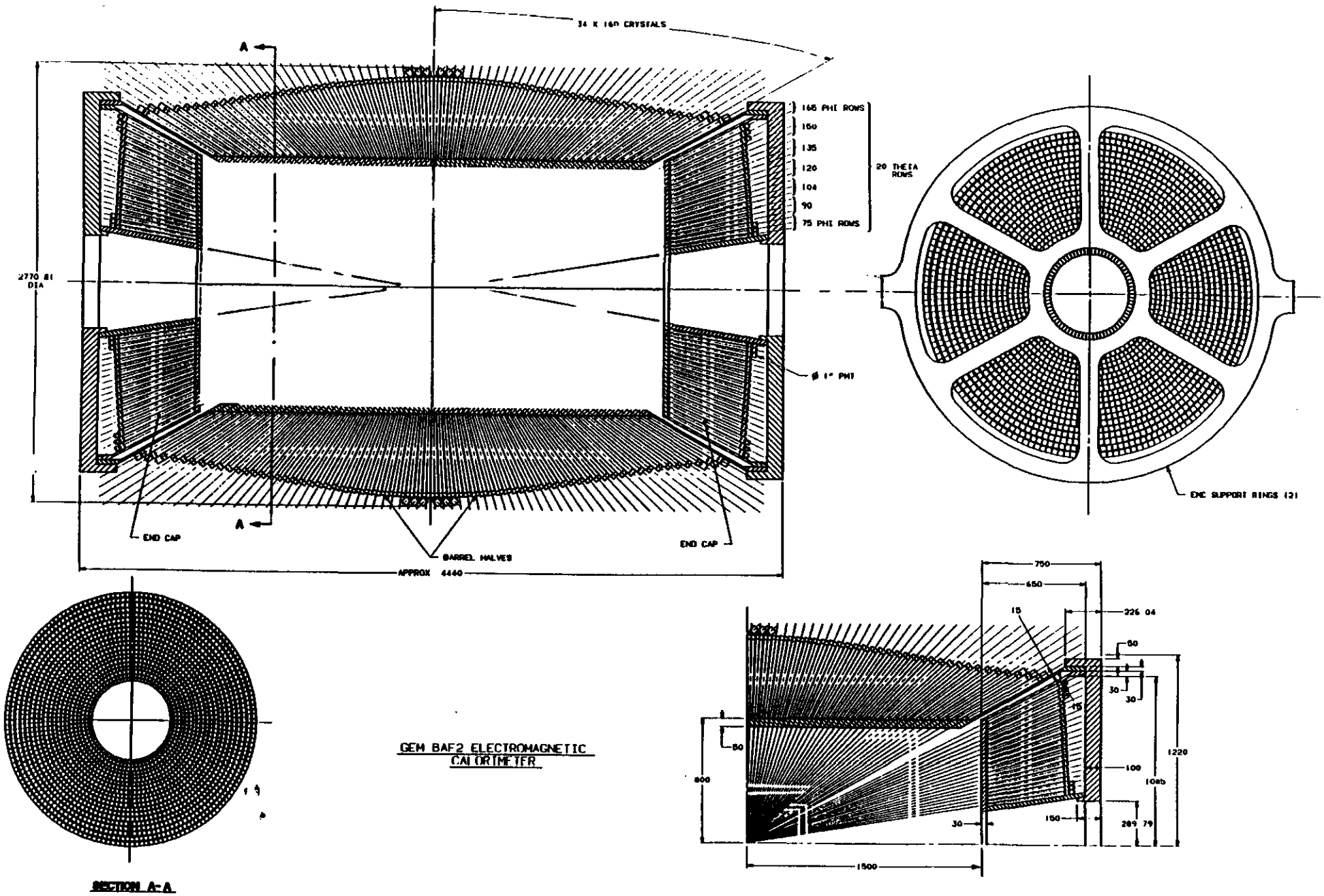

GEM Detector
Barium Fluoride EM Calorimeter

Figure 7

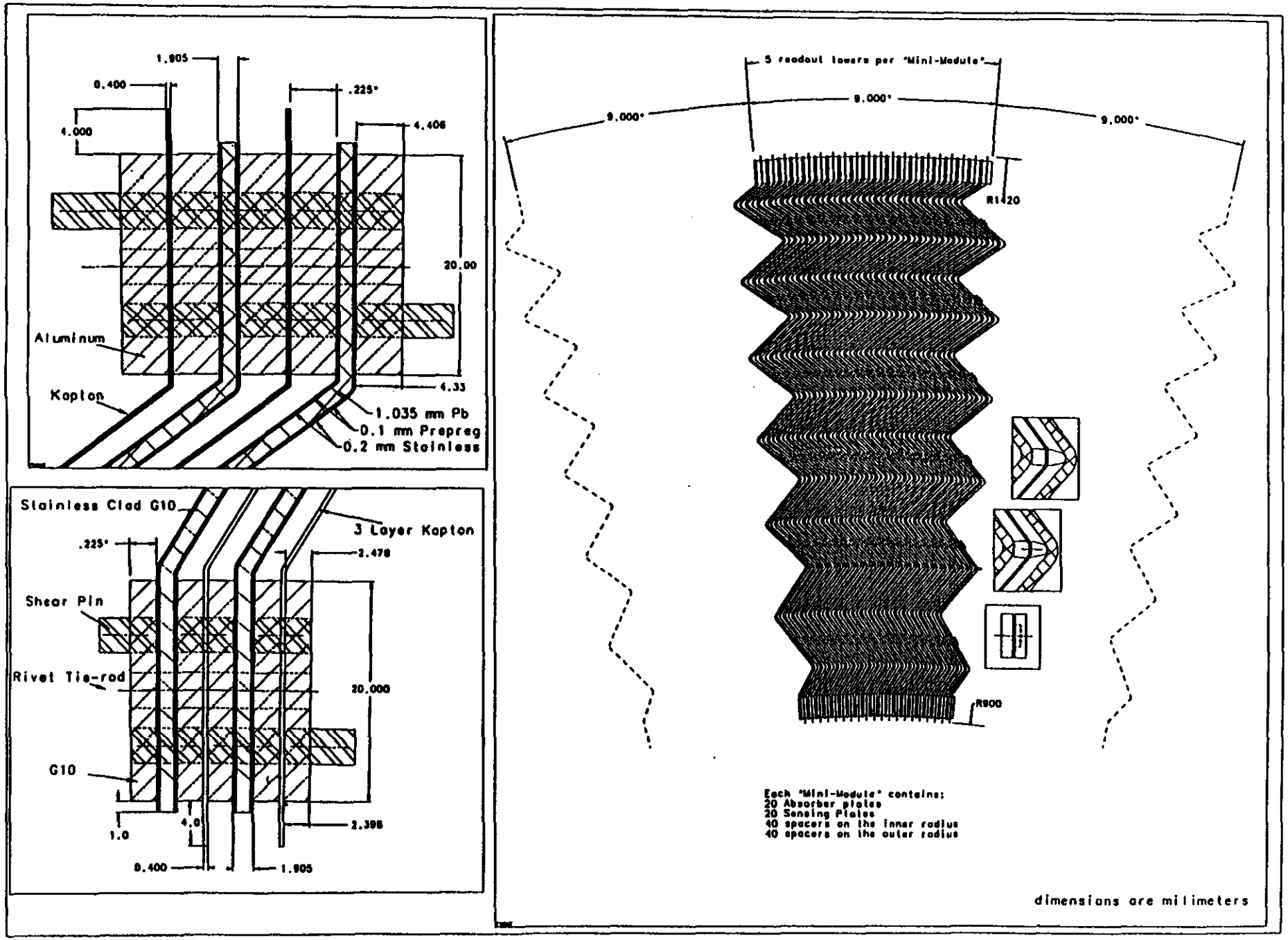

Accordion Mini-Module Barrel Section

Figure 8

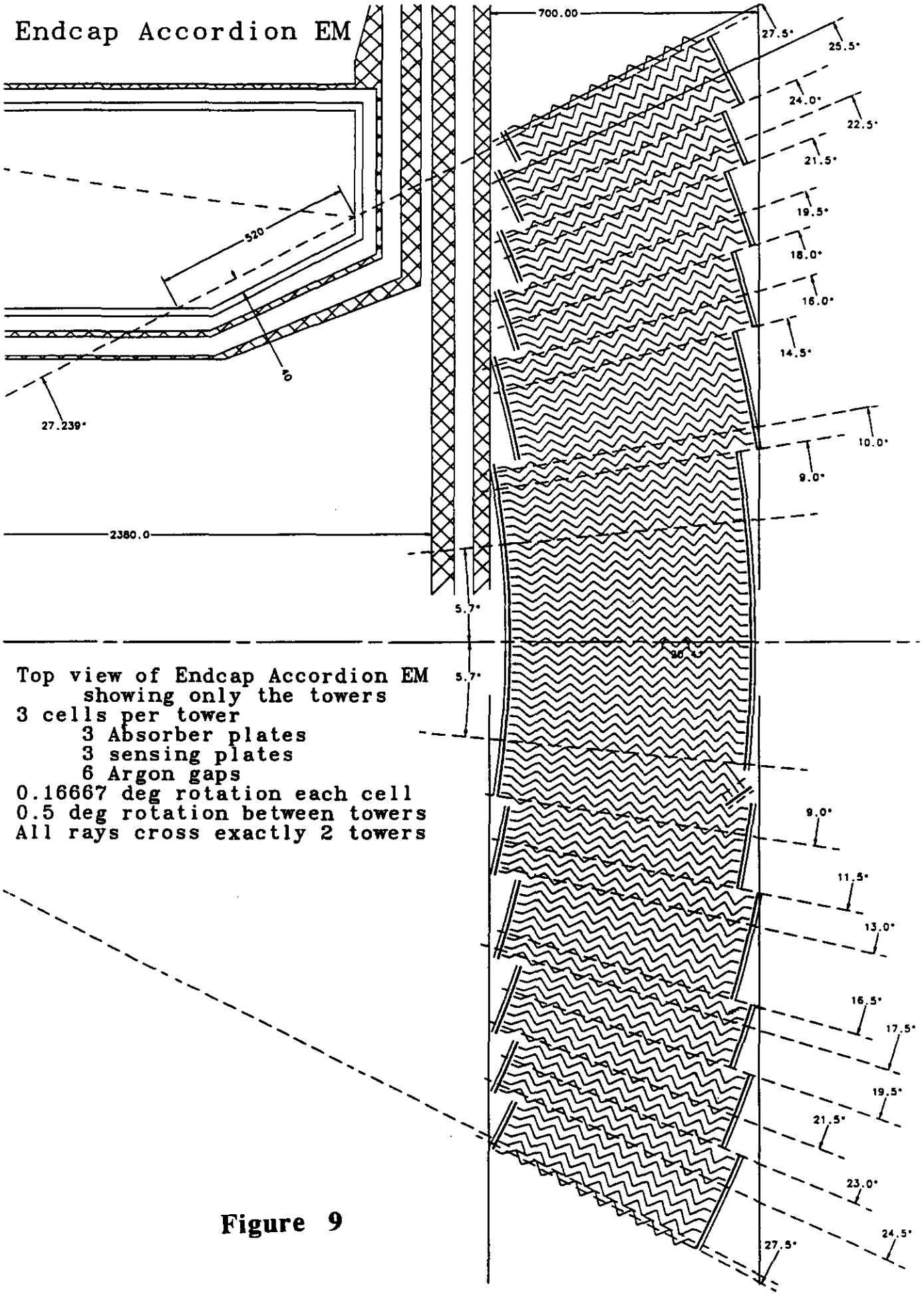
Endcap Accordion EM
700.00
520
27.239°
2380.0
5.7°
5.7°
27.5°
25.5°
24.0°
22.5°
21.5°
19.5°
18.0°
16.0°
14.5°
10.0°
9.0°
9.0°
11.5°
13.0°
16.5°
17.5°
19.5°
21.5°
23.0°
24.5°
27.5°
Top view of Endcap Accordion EM
showing only the towers
3 cells per tower
3 Absorber plates
3 sensing plates
6 Argon gaps
0.16667 deg rotation each cell
0.5 deg rotation between towers
All rays cross exactly 2 towers

Figure 9

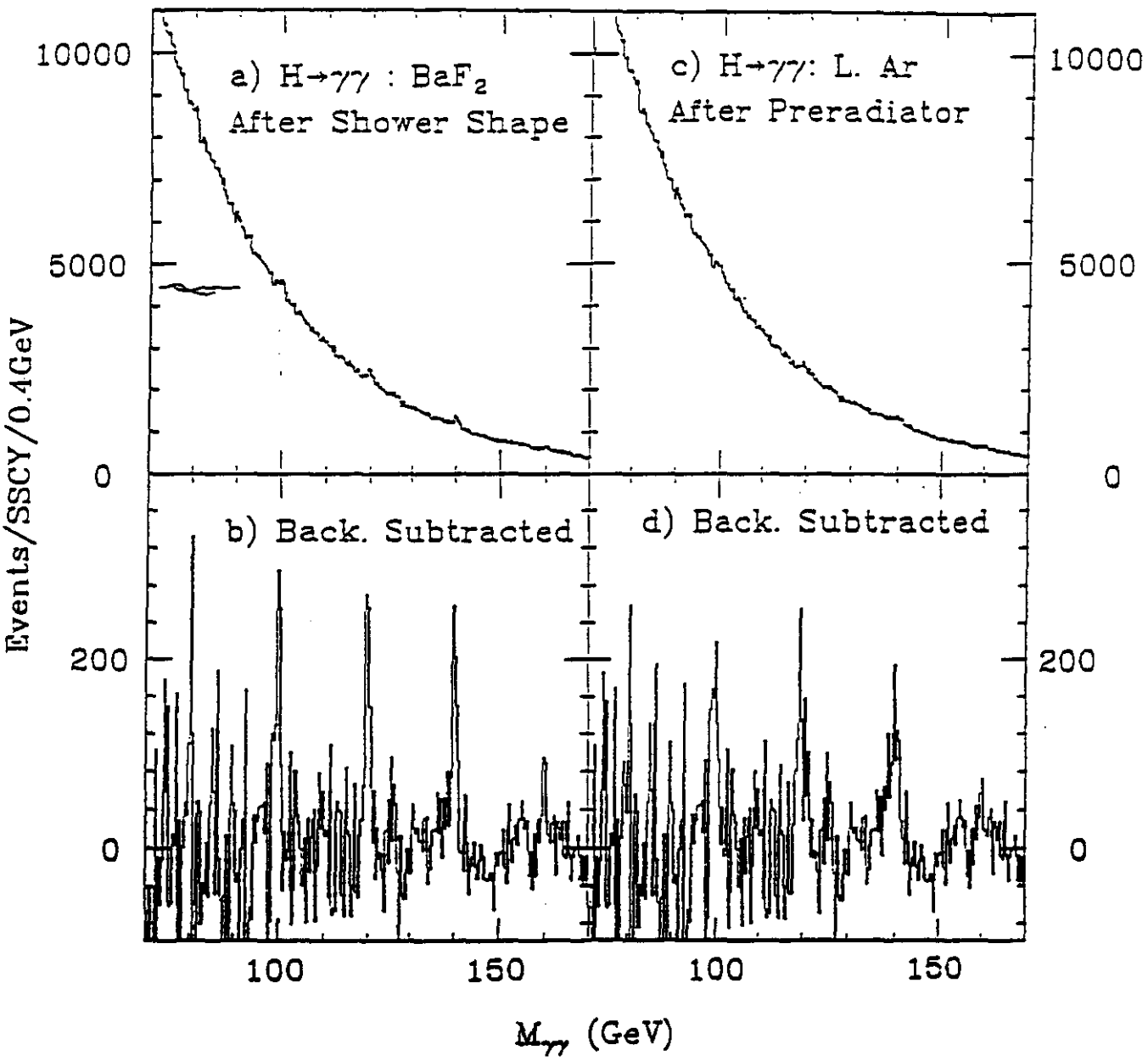
a) H→γγ : BaF2
After Shower Shape
c) H→γγ: L. Ar
After Preradiator
b) Back. Subtracted
d) Back. Subtracted
10000
5000
0
200
0
Events/SSCY/0.4GeV
100
150
100
150
Mγγ (GeV)

Figure 10

LIQUID ARGON CALORIMETER - 12 X 14 LAMBDA, FLAT ENDCAP HEAD

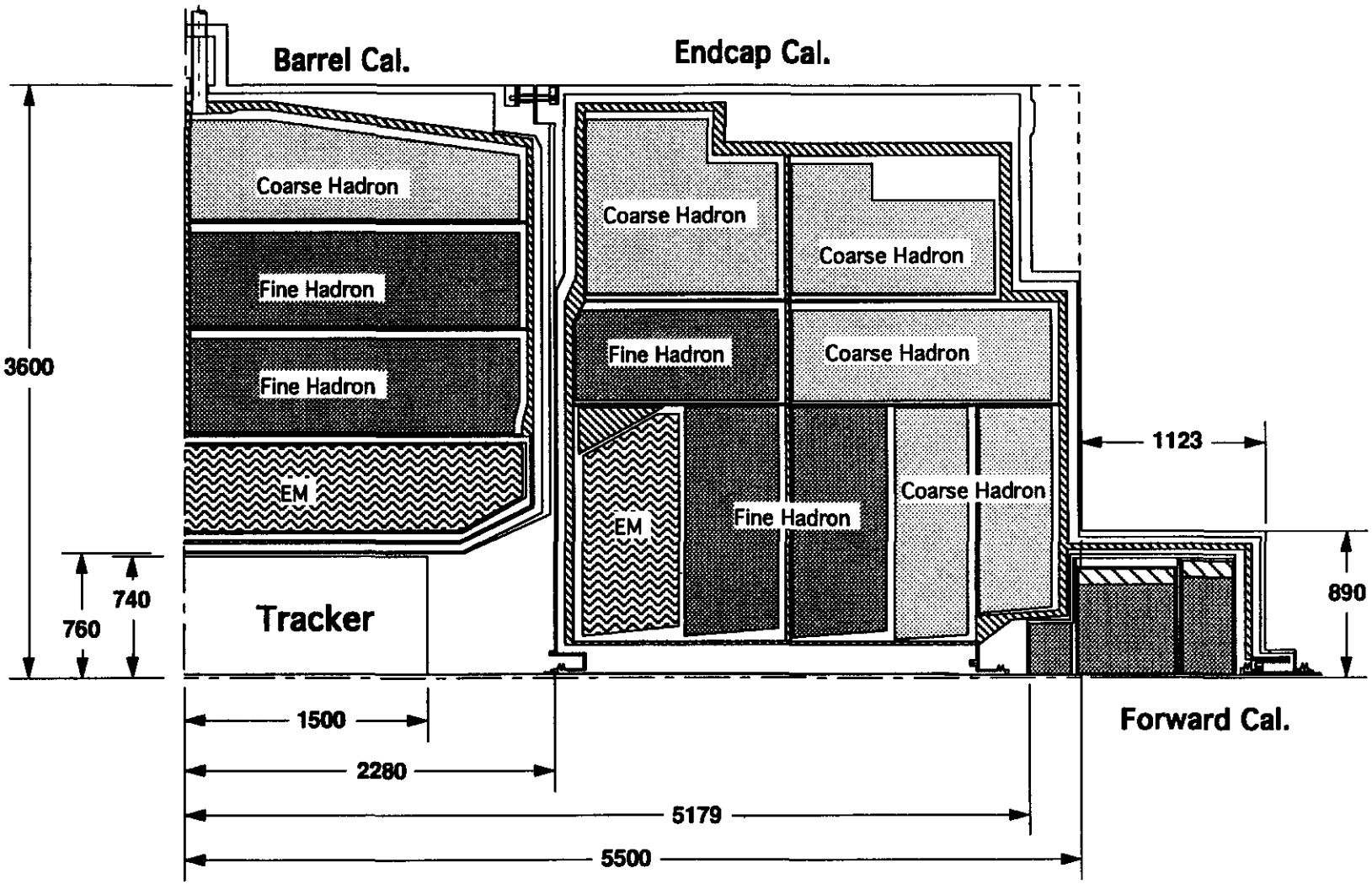

Figure 11

Dimensions in millimeters

LLMASON 920620 BASELINE.LAC

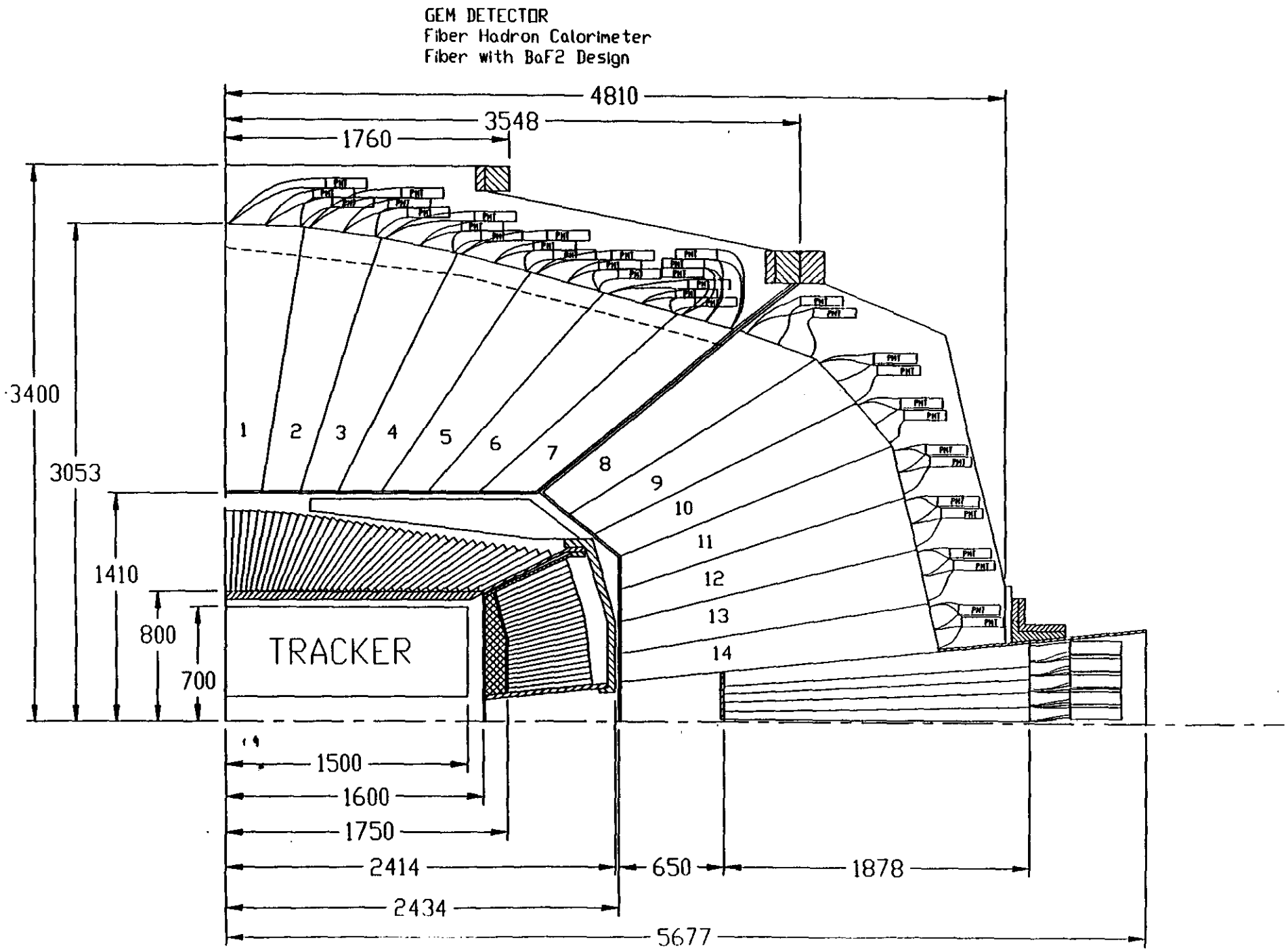
GEM DETECTOR
Fiber Hadron Calorimeter
Fiber with BaF2 Design
4810
3548
1760
3400
3053
1410
800
700
TRACKER
1
2
3
4
5
6
7
8
9
10
11
12
13
14
1500
1600
1750
2414
650
1878
2434
5677

Figure 12

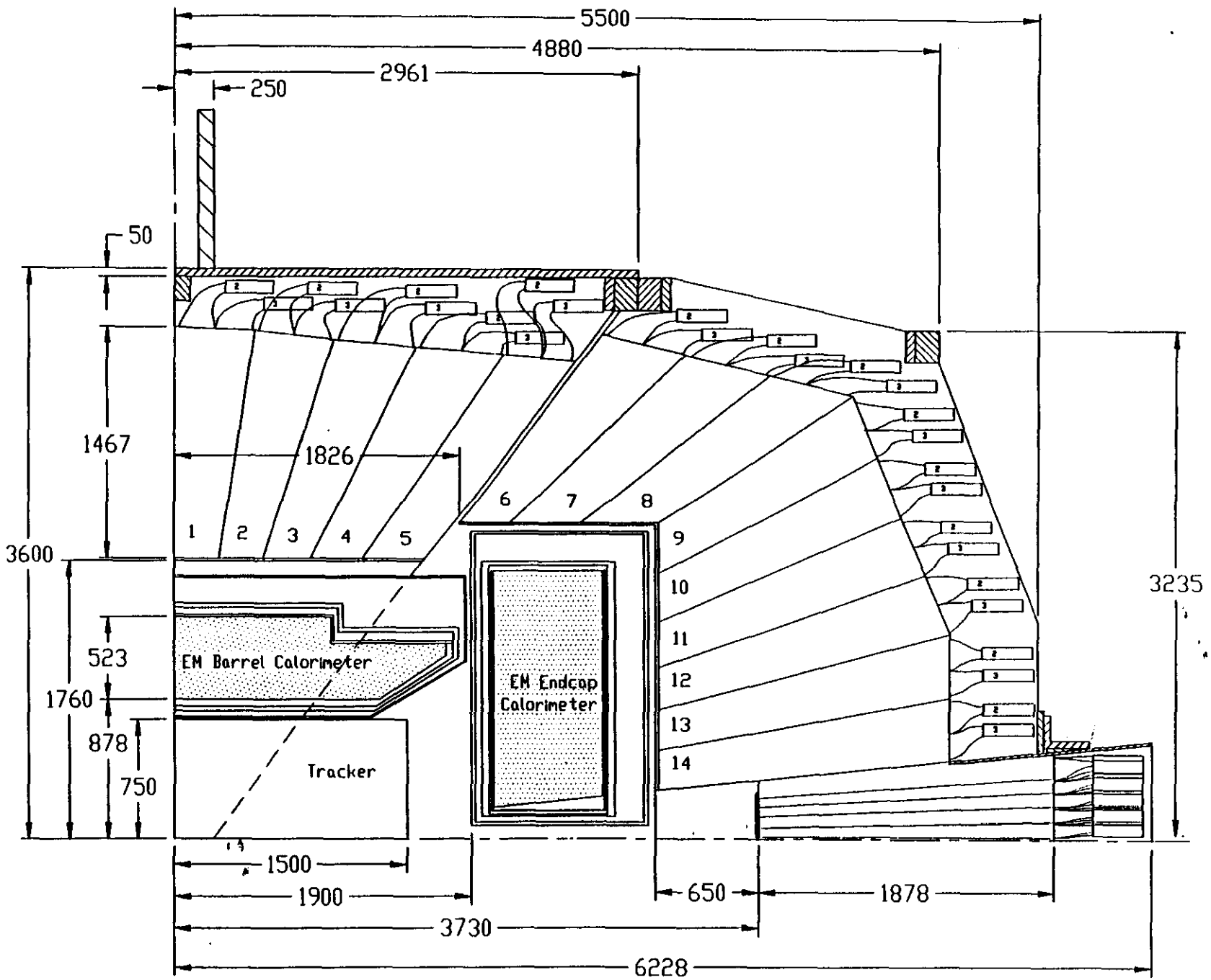

Figure 13

GEM DETECTOR
Fiber Hadron Calorimeter
Fiber with Current LKr Design

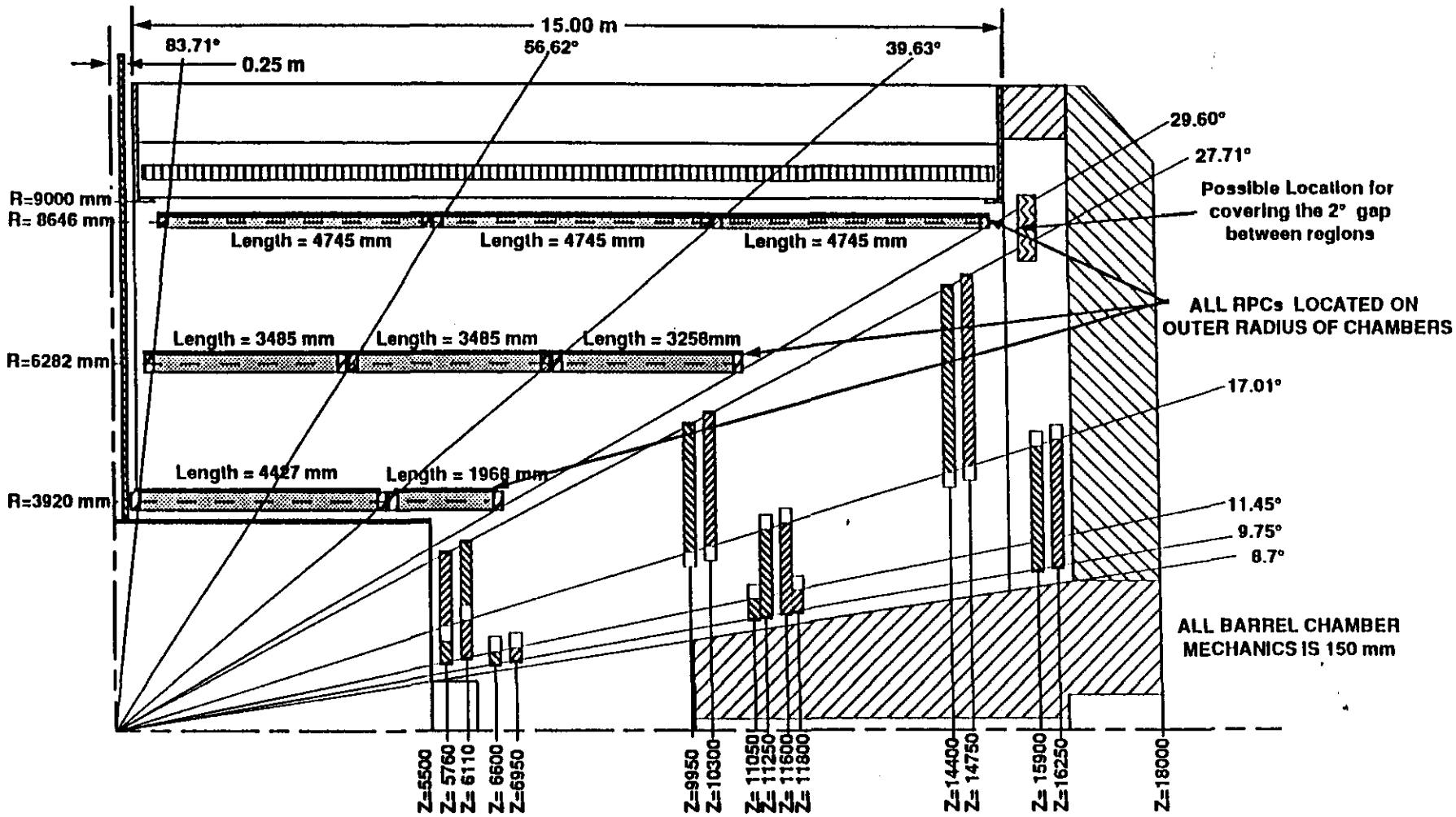

GEM MUON SYSTEM CHAMBER LAYOUT
BASELINE II
(2,3,3 Chambers per Layer-PROJECTIVE GAPS)

Draper Laboratory	
GEM Muon System Chamber Layout	
Drawn By: F. Nimblett	Rev (-)
Dwg. No: GMU0015	6/30/92
Approved by:	

Figure 14

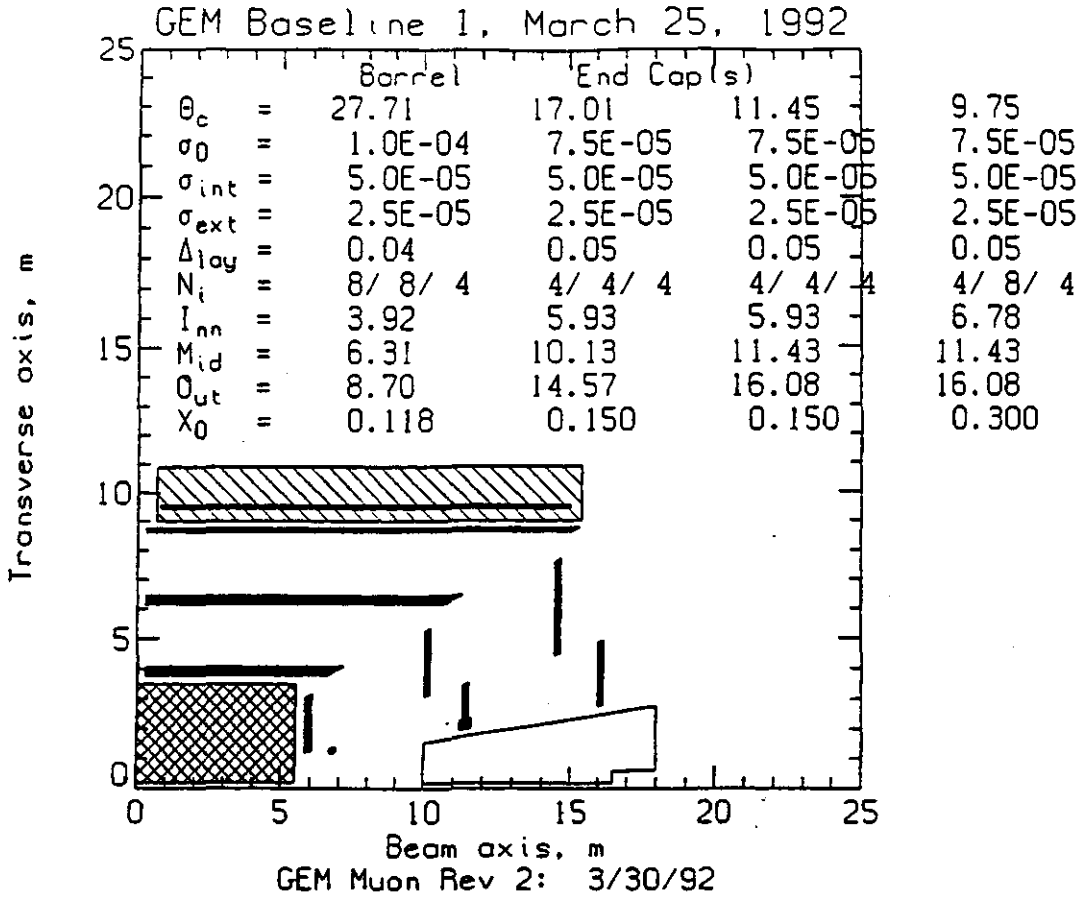
GEM Baseline 1, March 25, 1992
Barrel
End Cap(s)
θc = 27.71 17.01 11.45 9.75
σ0 = 1.0E-04 7.5E-05 7.5E-05 7.5E-05
σint = 5.0E-05 5.0E-05 5.0E-05 5.0E-05
σext = 2.5E-05 2.5E-05 2.5E-05 2.5E-05
Δlay = 0.04 0.05 0.05 0.05
Ni = 8/ 8/ 4 4/ 4/ 4 4/ 4/ 4 4/ 8/ 4
Inn = 3.92 5.93 5.93 6.78
Mid = 6.31 10.13 11.43 11.43
Out = 8.70 14.57 16.08 16.08
X0 = 0.118 0.150 0.150 0.300
Transverse axis, m
Beam axis, m
GEM Muon Rev 2: 3/30/92

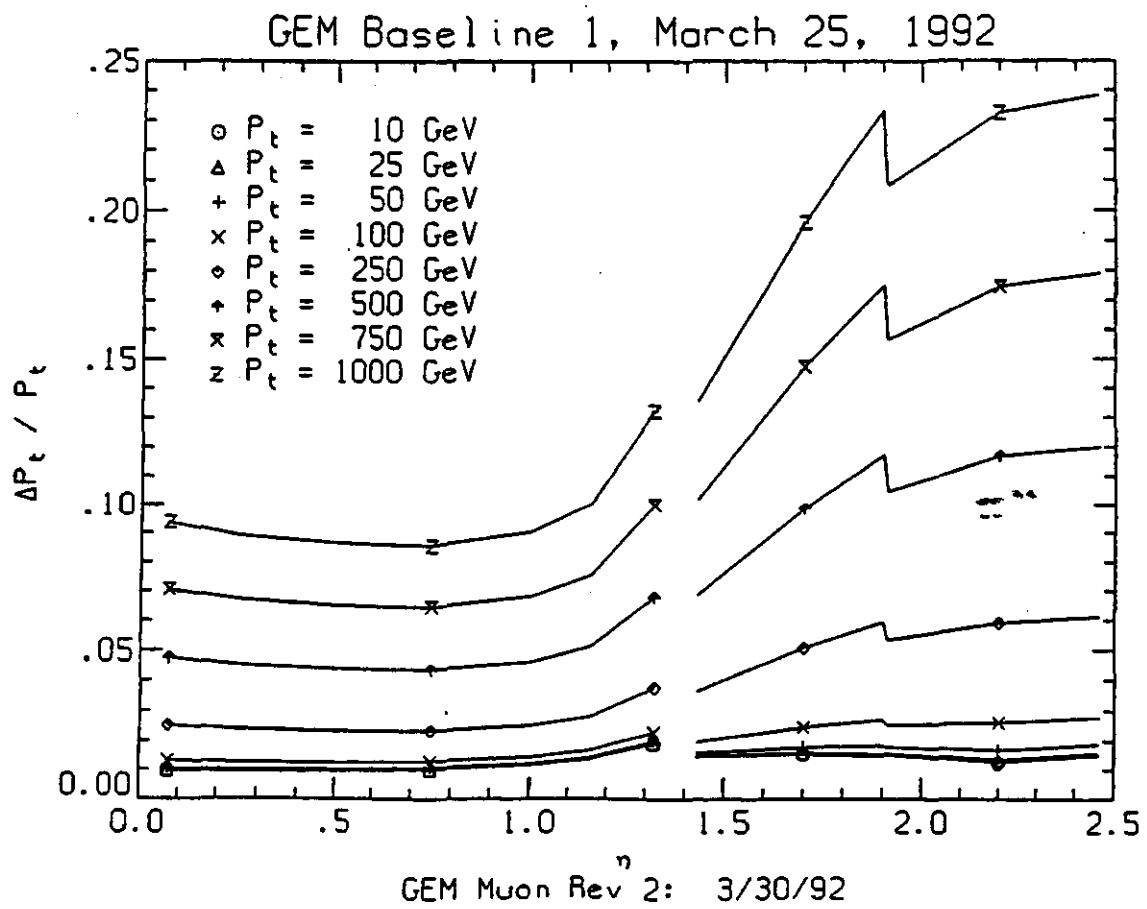
GEM Baseline 1, March 25, 1992
Pt = 10 GeV
Pt = 25 GeV
Pt = 50 GeV
Pt = 100 GeV
Pt = 250 GeV
Pt = 500 GeV
Pt = 750 GeV
Pt = 1000 GeV
ΔPt / Pt
η
GEM Muon Rev 2: 3/30/92

Figure 15

Prototype Cathode Strip Chamber

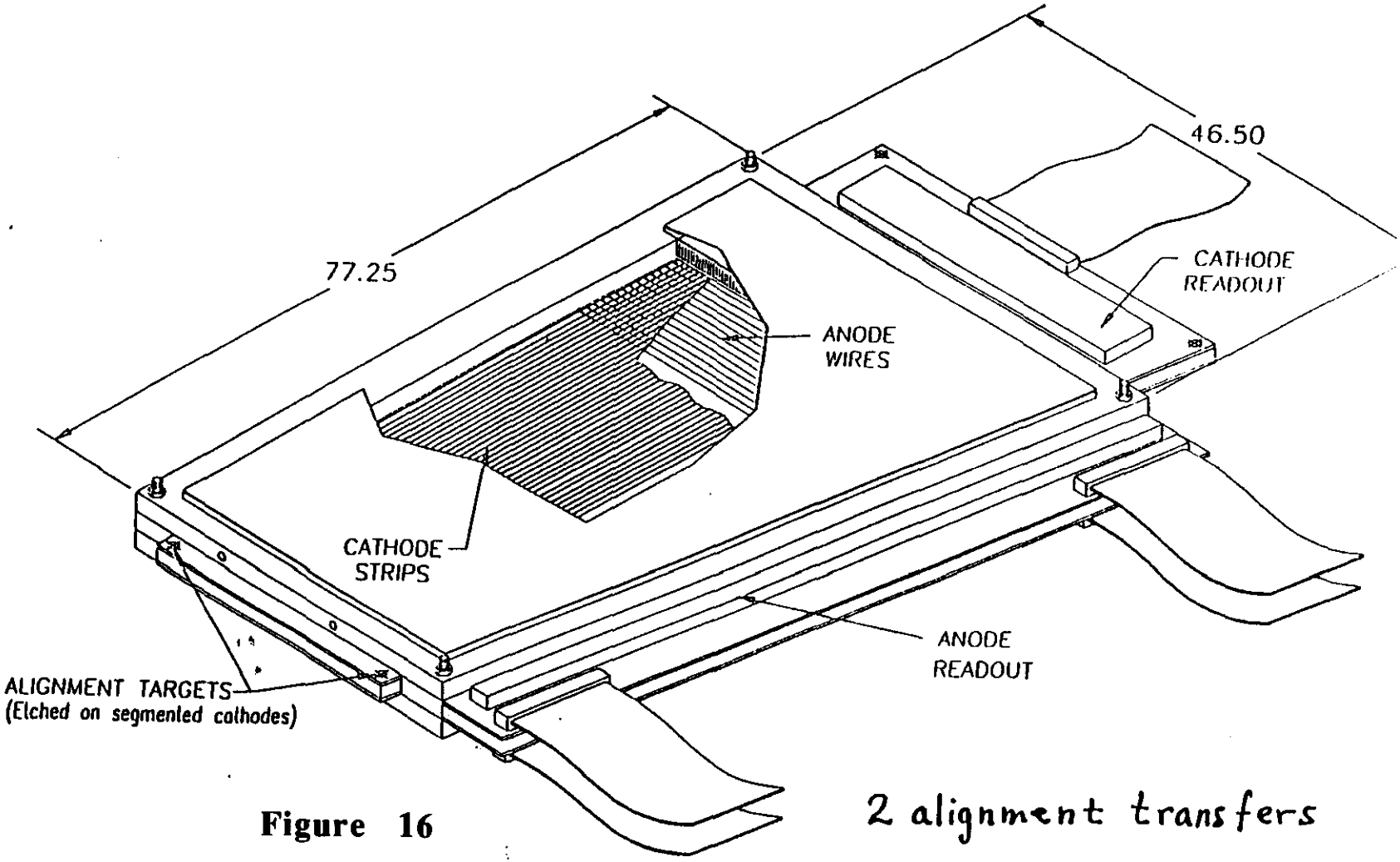

Figure 16

2 alignment transfers

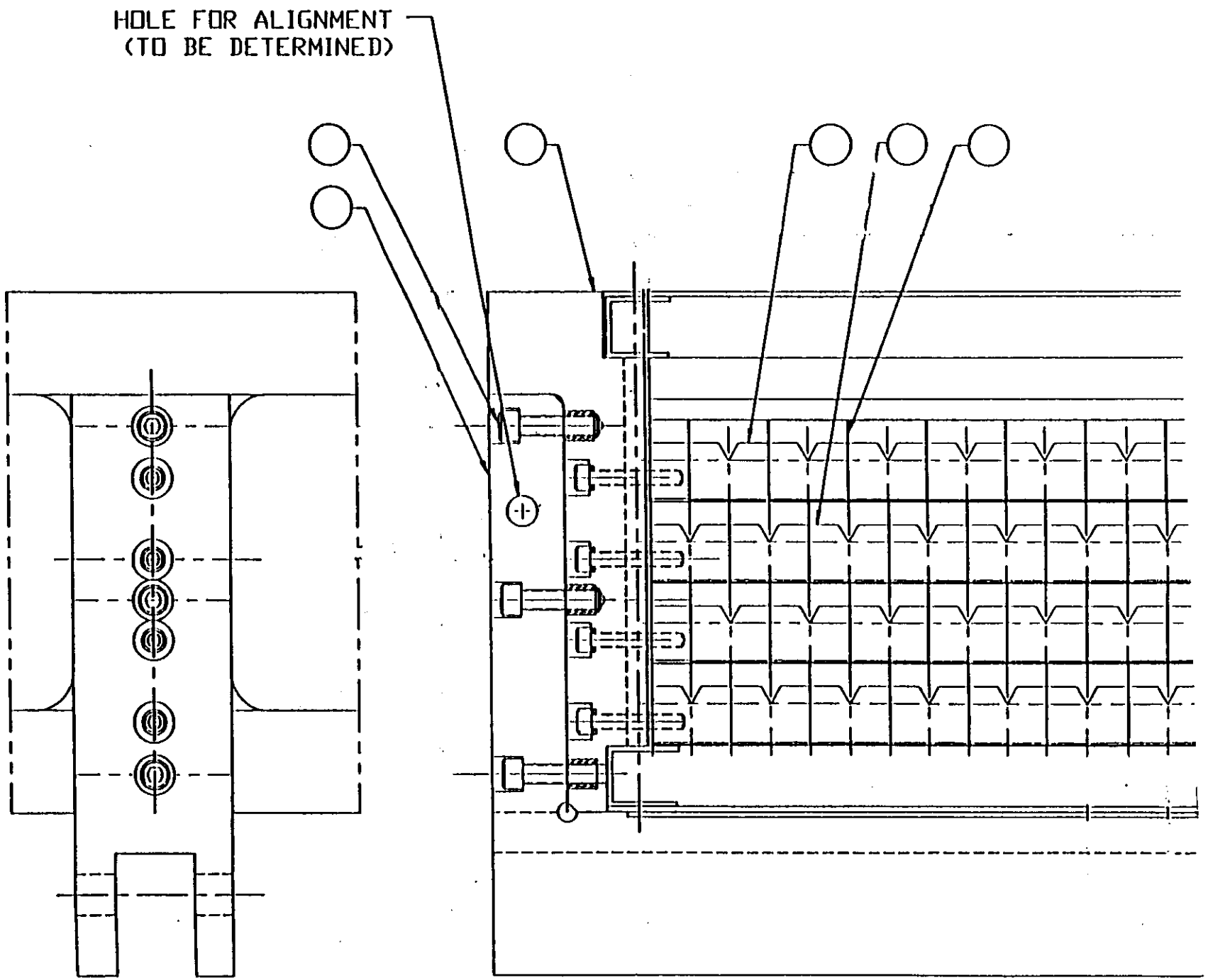

Figure 17

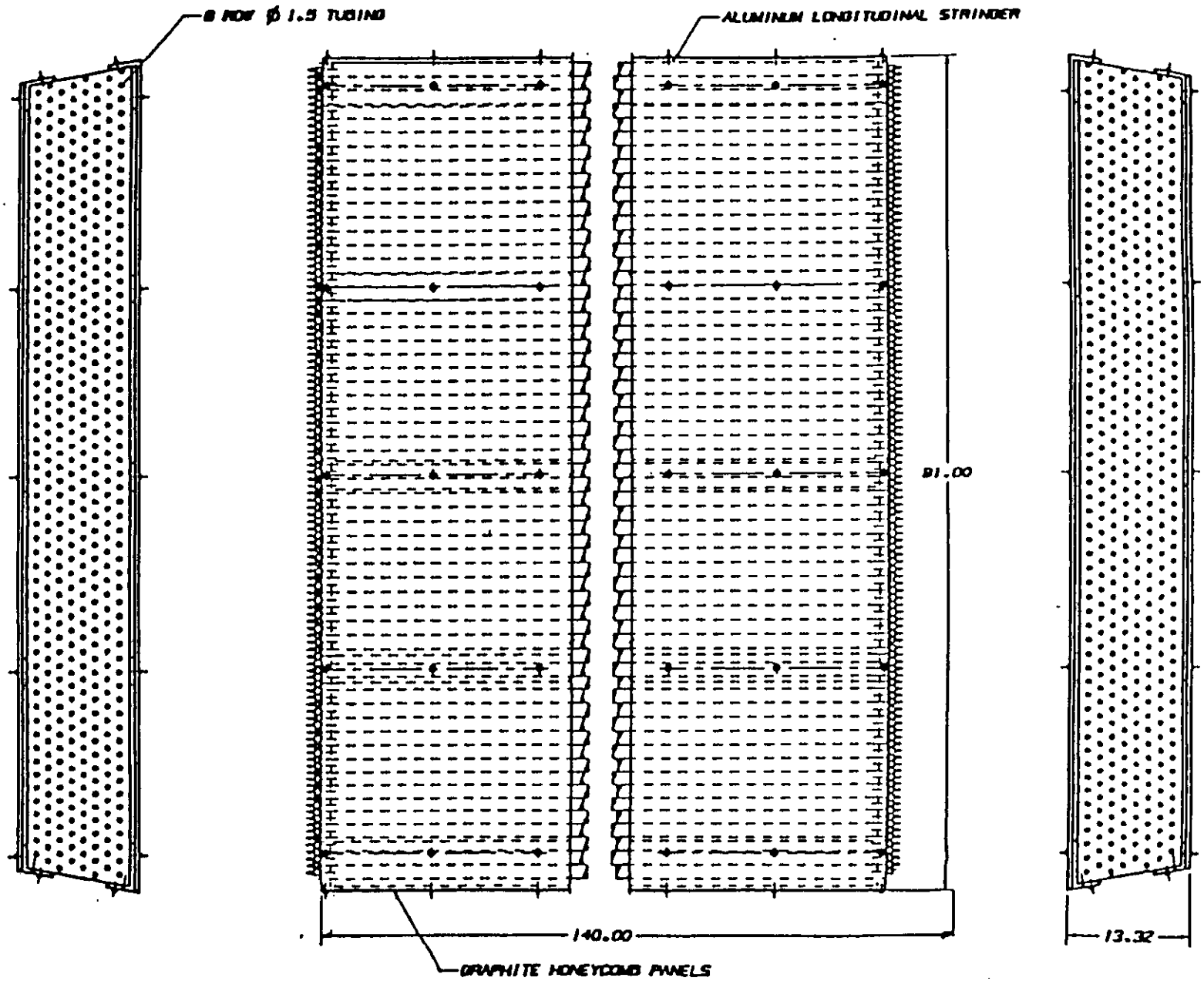
8 ROW Ø 1.5 TUBING
ALUMINUM LONGITUDINAL STRINGER
91.00
140.00
13.32
GRAPHITE HONEYCOMB PANELS

Figure 18

Outer Cermet RPC cross section and weight calculation: total thickness = 3 cm

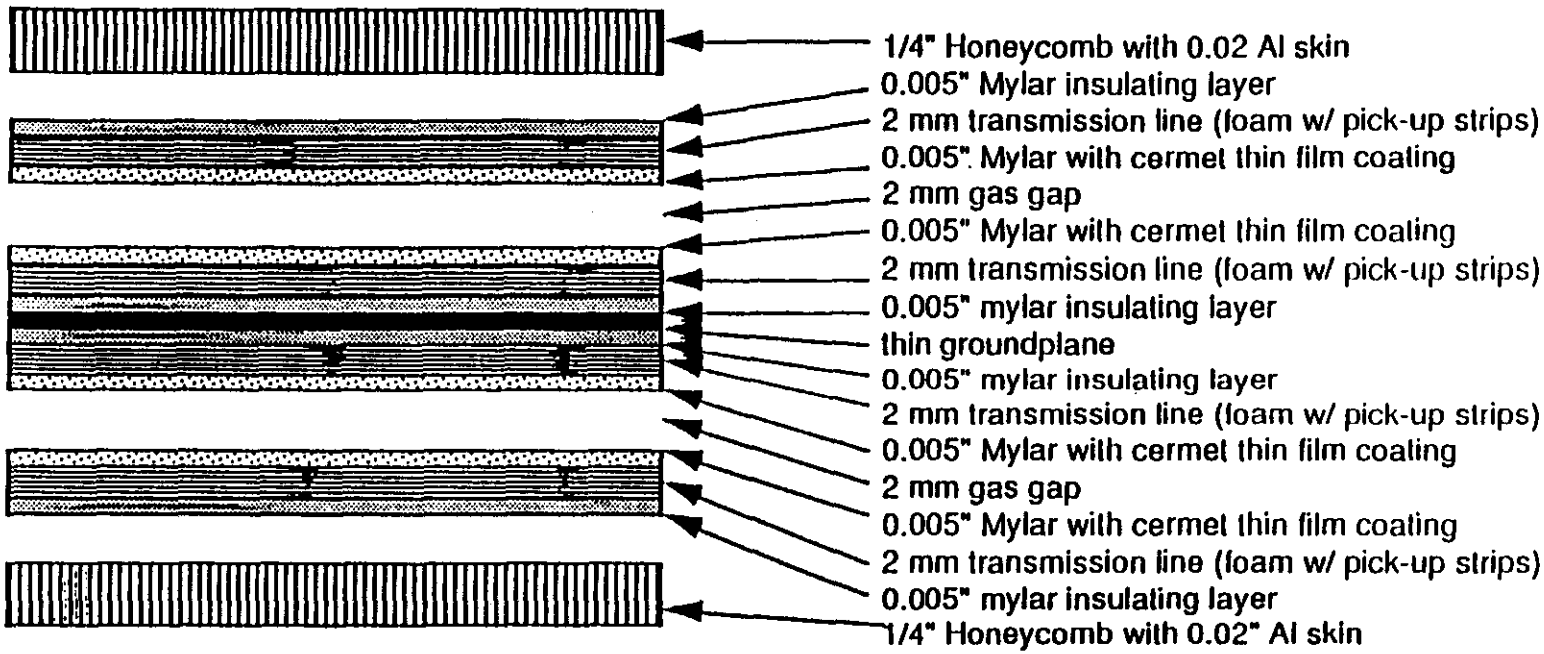

Densities: Coated Mylar and all materials except Honeycomb and foam = 1.5 g/cm**3
Honeycomb = 0.435 g/cm**2 (7.9 lb/cu. ft., 1/4" thick with 0.02" aluminum skins)
Foam = 0.2 g/cm**3

Areal Mass of two layer RPC = 2 x (0.435 g/cm**2) + 0.102 cm x (1.5 g/cm**3) + 0.8 cm x (0.2 g/cm**3)
= 1.18 g/cm**2 = 1.68 x 10**-2 psi

For four 380 cm x 329.6 cm outer sector chambers:

4 x (380 cm x 329.6 cm) x 1 in**2/(2.54 cm)**2 x 1.68 x 10**-2 psi = 1305 lb

Aluminum U-channel framework: U-channel @ 3.81 cm H x 5 cm W with 0.159 cm thick ribs, 2.14 cm**2 cross section

4 x ((380 cm x 2) + (329.6 cm x 2)) = 5677 cm perimeter

5677 cm x 2.14 cm**2 x 2.7 g/cm**3 x 2.205 lb/1000 g = 72.3 lb

Figure 19

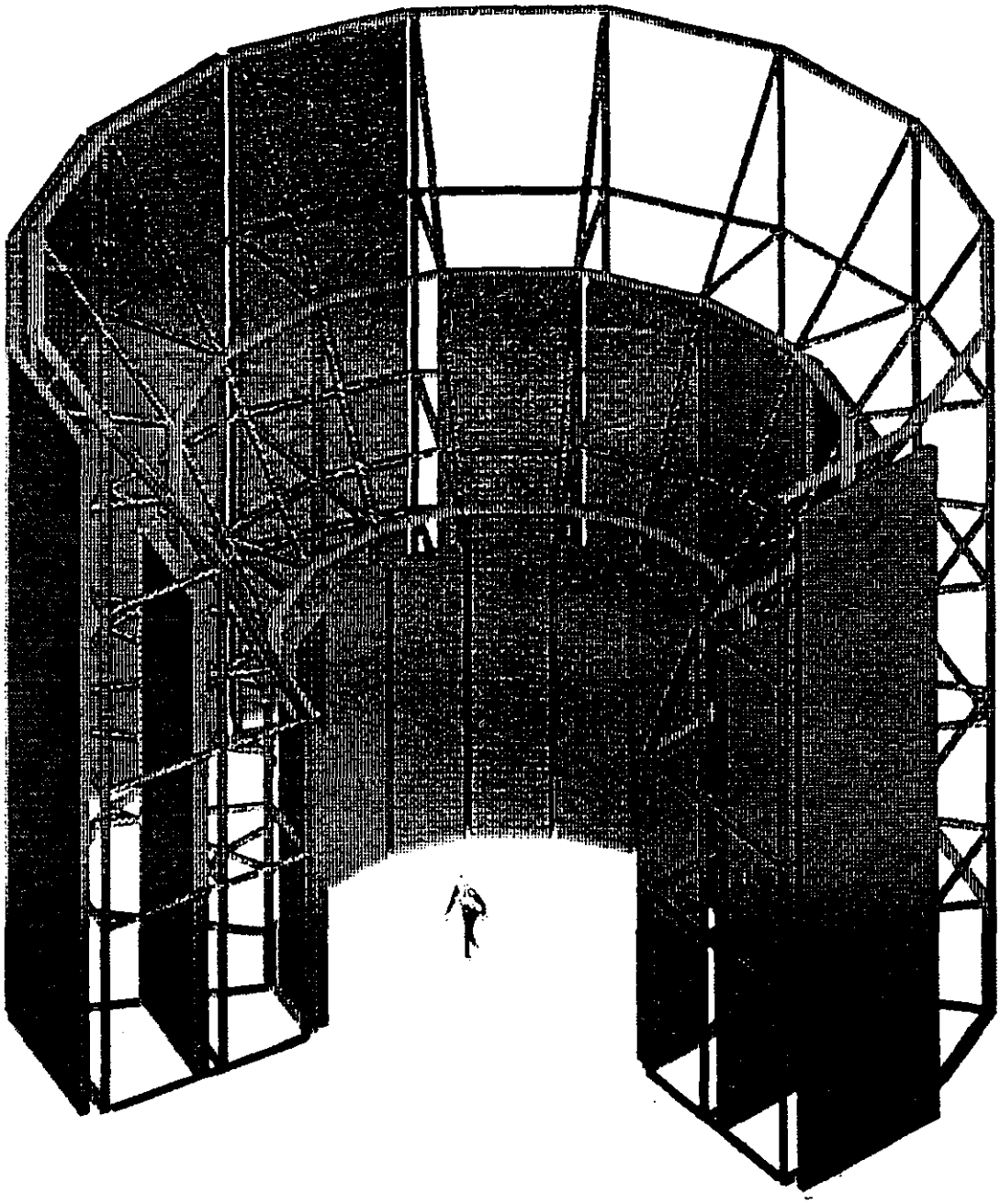

Figure 20

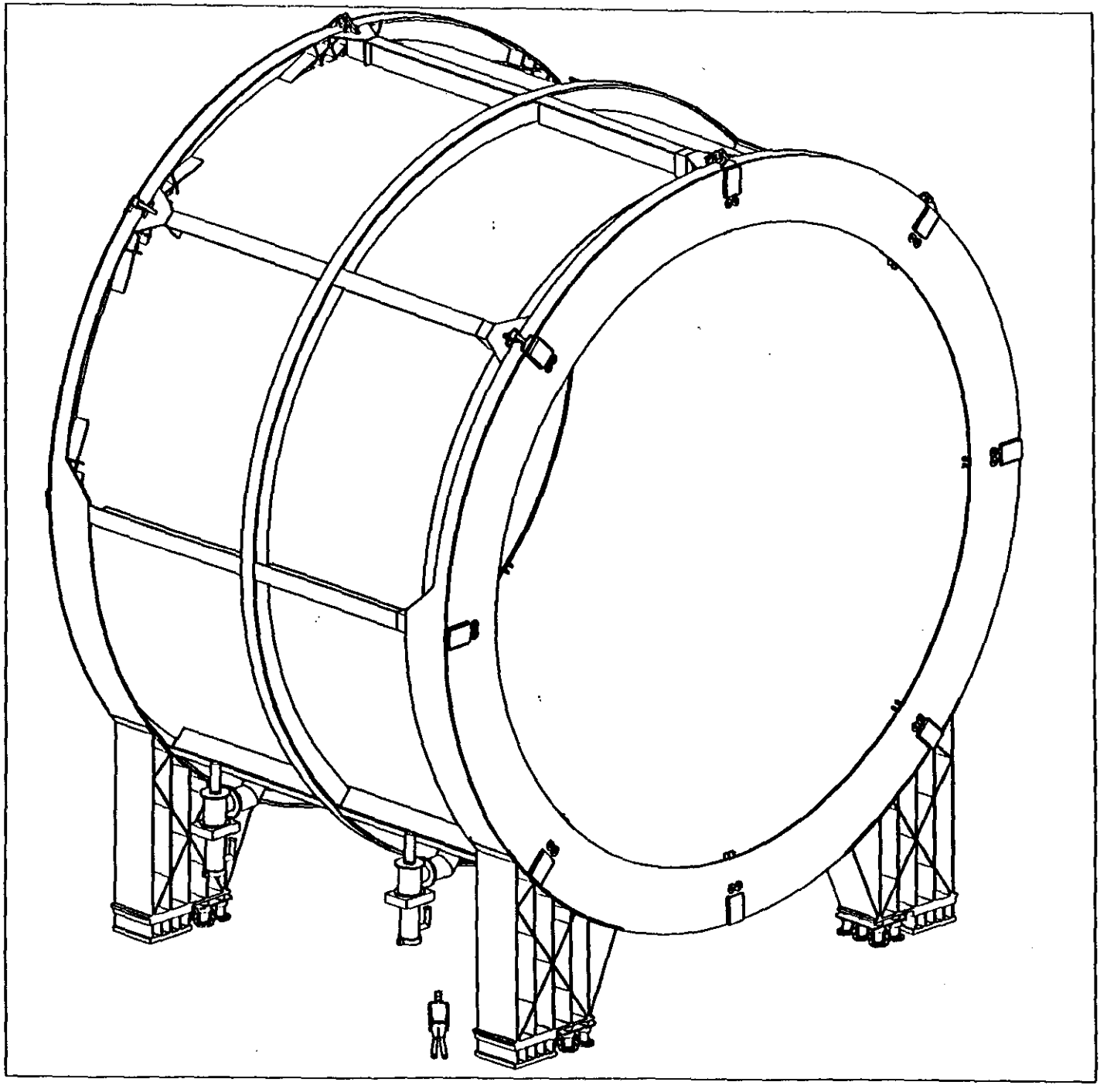

Figure 21

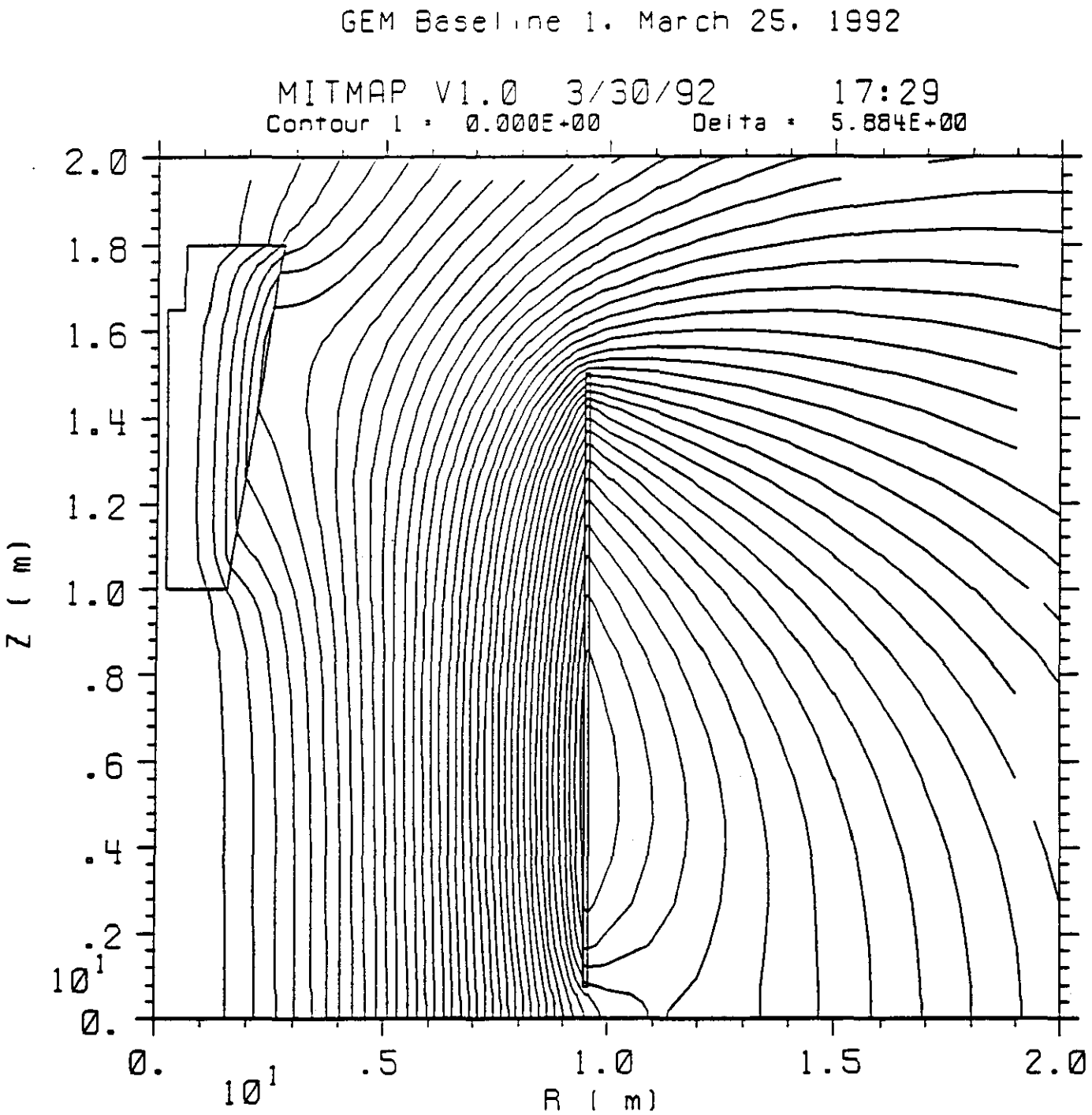

CONTOURS OF CONSTANT FLUX

Figure 1: Lines of constant magnetic flux in a meridional half-plane; the figure is rotationally symmetric about the horizontal axis and has mirror symmetry about $Z = 0$. Note: the beam axis, Z, is vertical while the transverse axis, R is horizontal. Both axes extend from 0 to 20 m and the field is in gauss. A sketch of the superconducting winding and the forward field shaper is also shown.

Figure 22

Design and analysis by Brian Smith, LANL

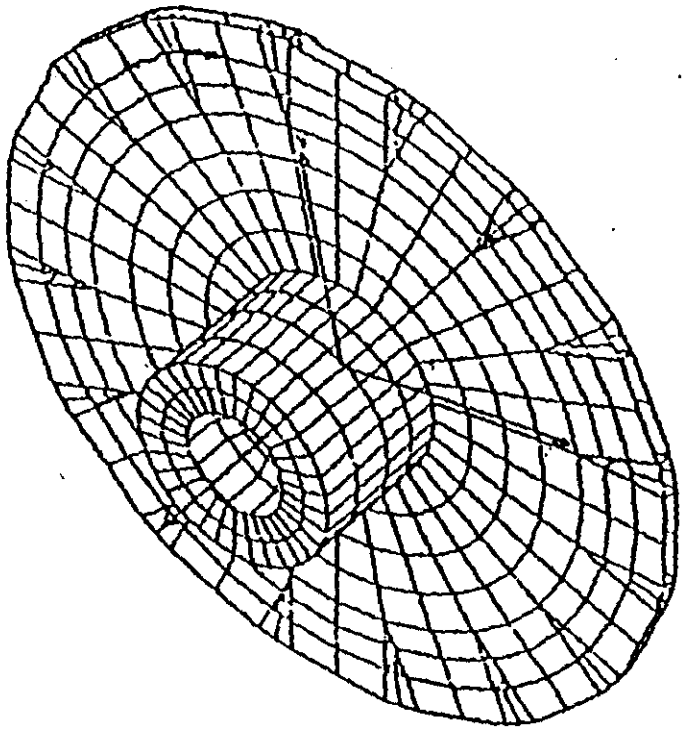

Model of full membrane concept

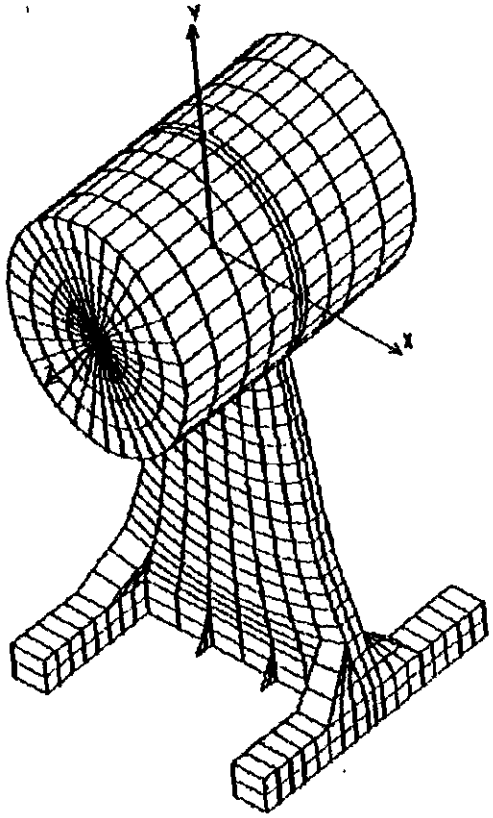

Model of pedestal support concept

Figure 23

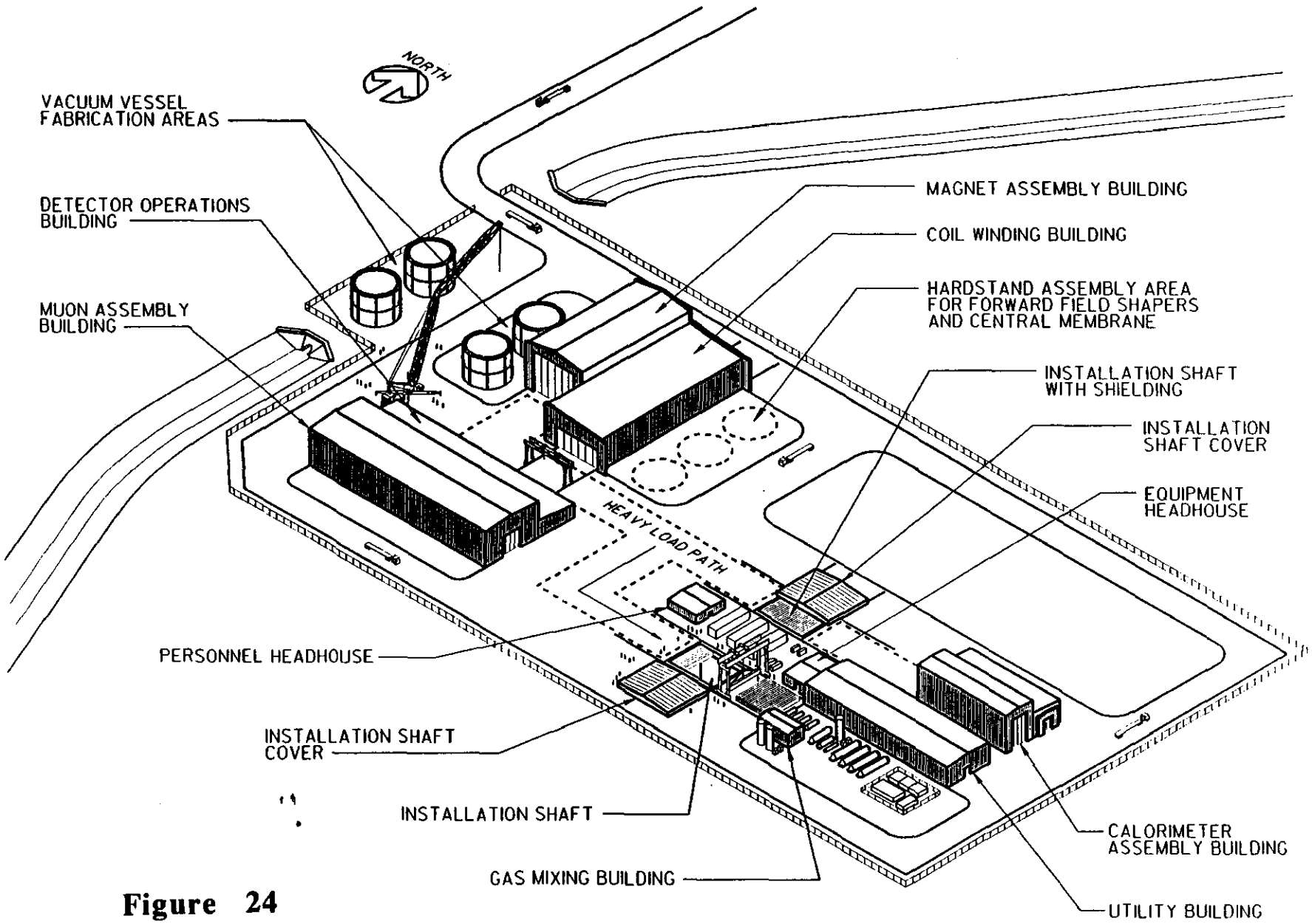

Figure 24

IR-5 SITE

TVP/kh/hh - 5/20/92 - GCD000157.BW

GEM EXPERIMENTAL HALL - CABLE SHAFT SIDE

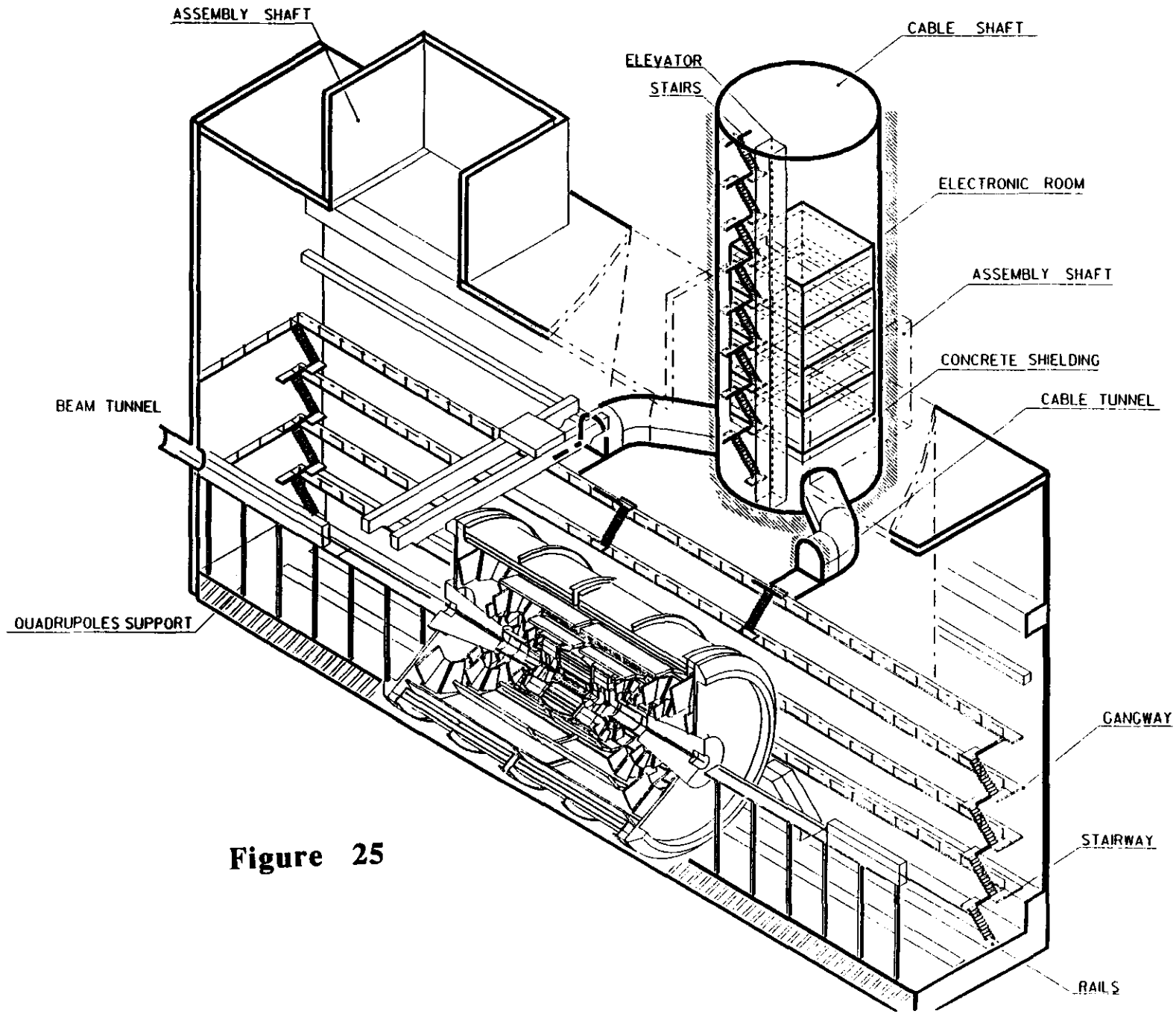

Figure 25

csect1
jun-25-92

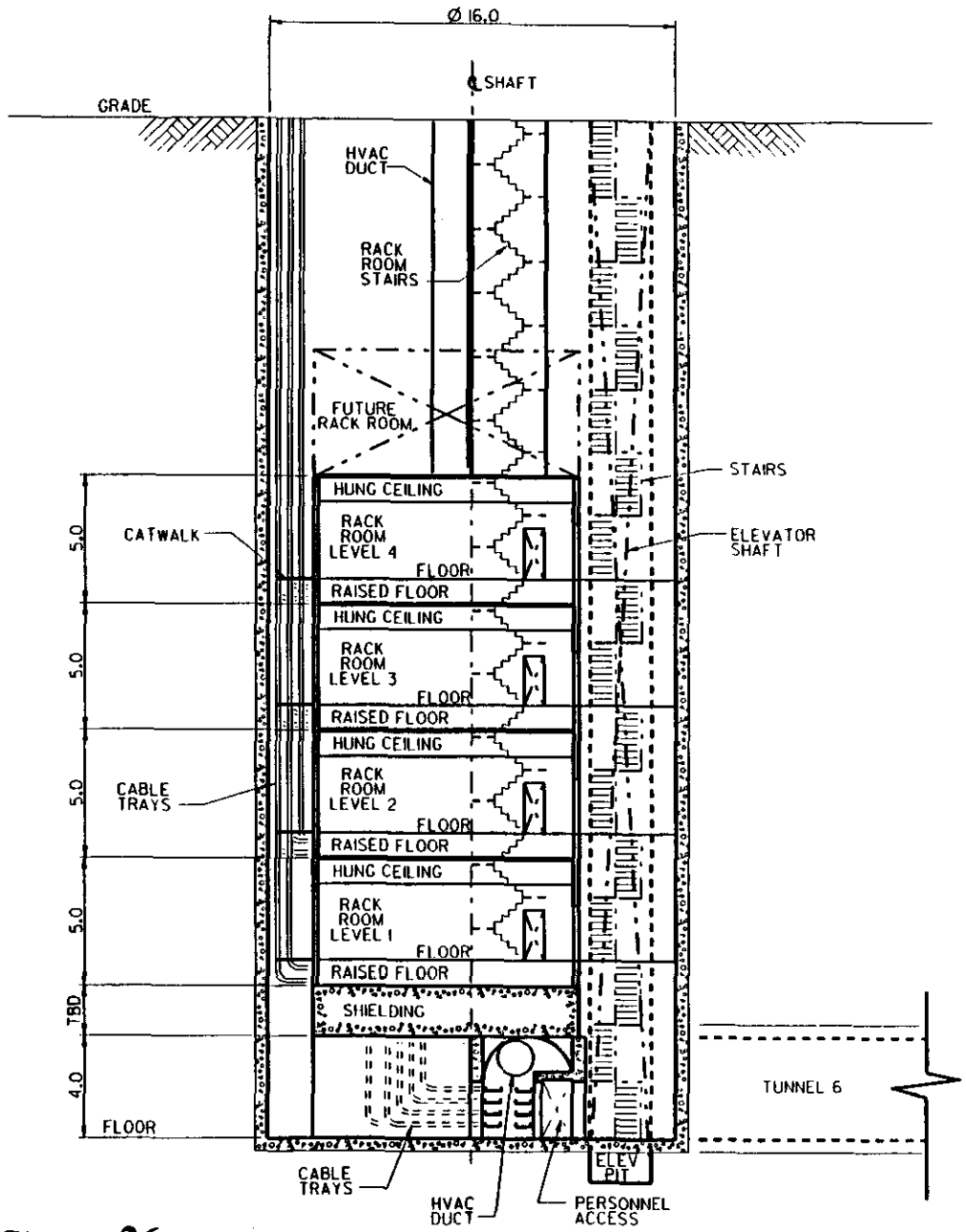

Figure 26

SECTION A-A
CABLE ELECTRONICS SHAFT

PHASE 3
INSTALL MAGNET HALF COIL SOUTH

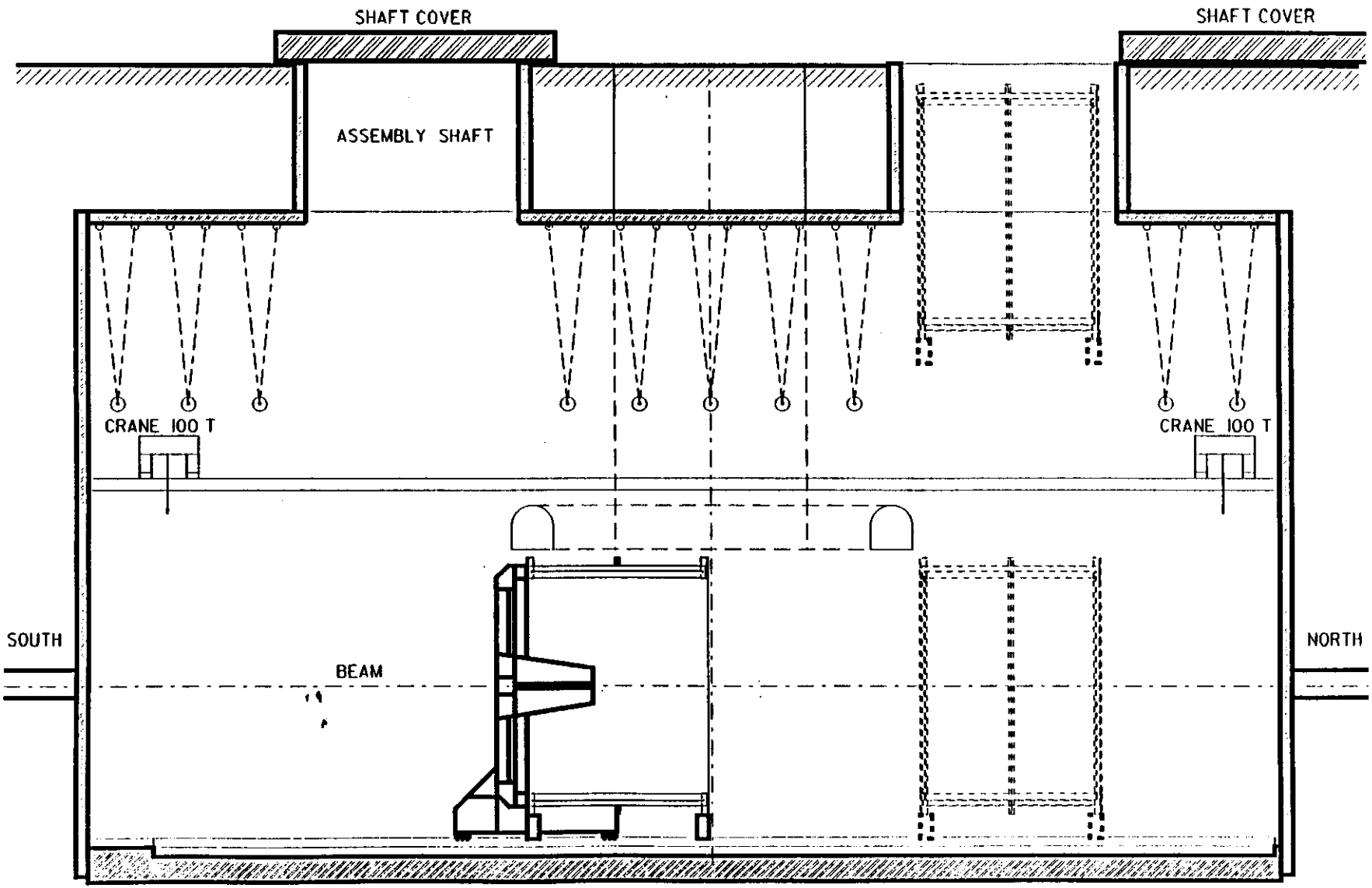

Figure 27

PHASE 6
INSTALL FORWARD FIELD SHAPER NORTH

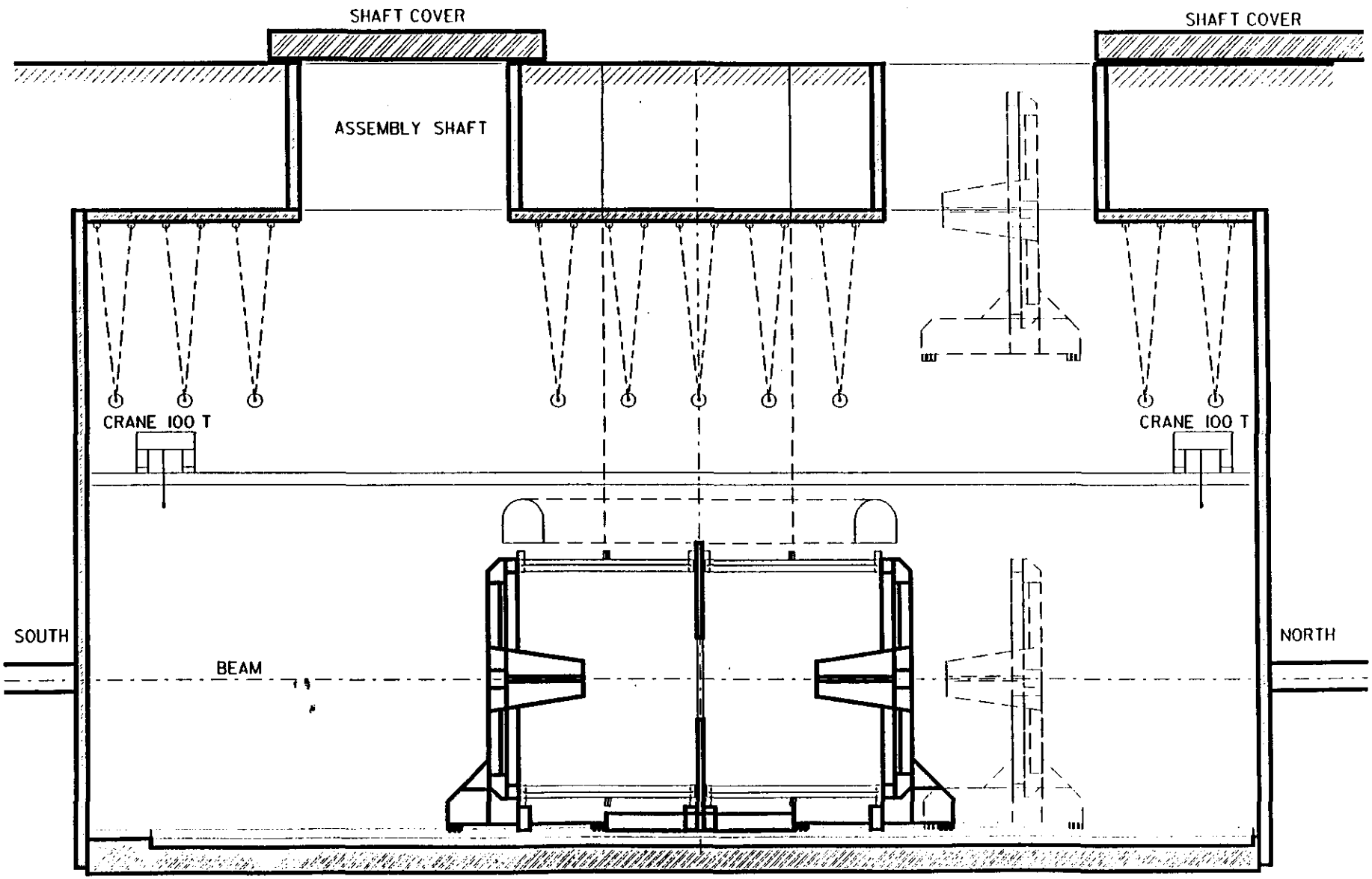

Figure 28

PHASE 10
INSTALL MUON BARREL SOUTH - END CAP CALORIMETER

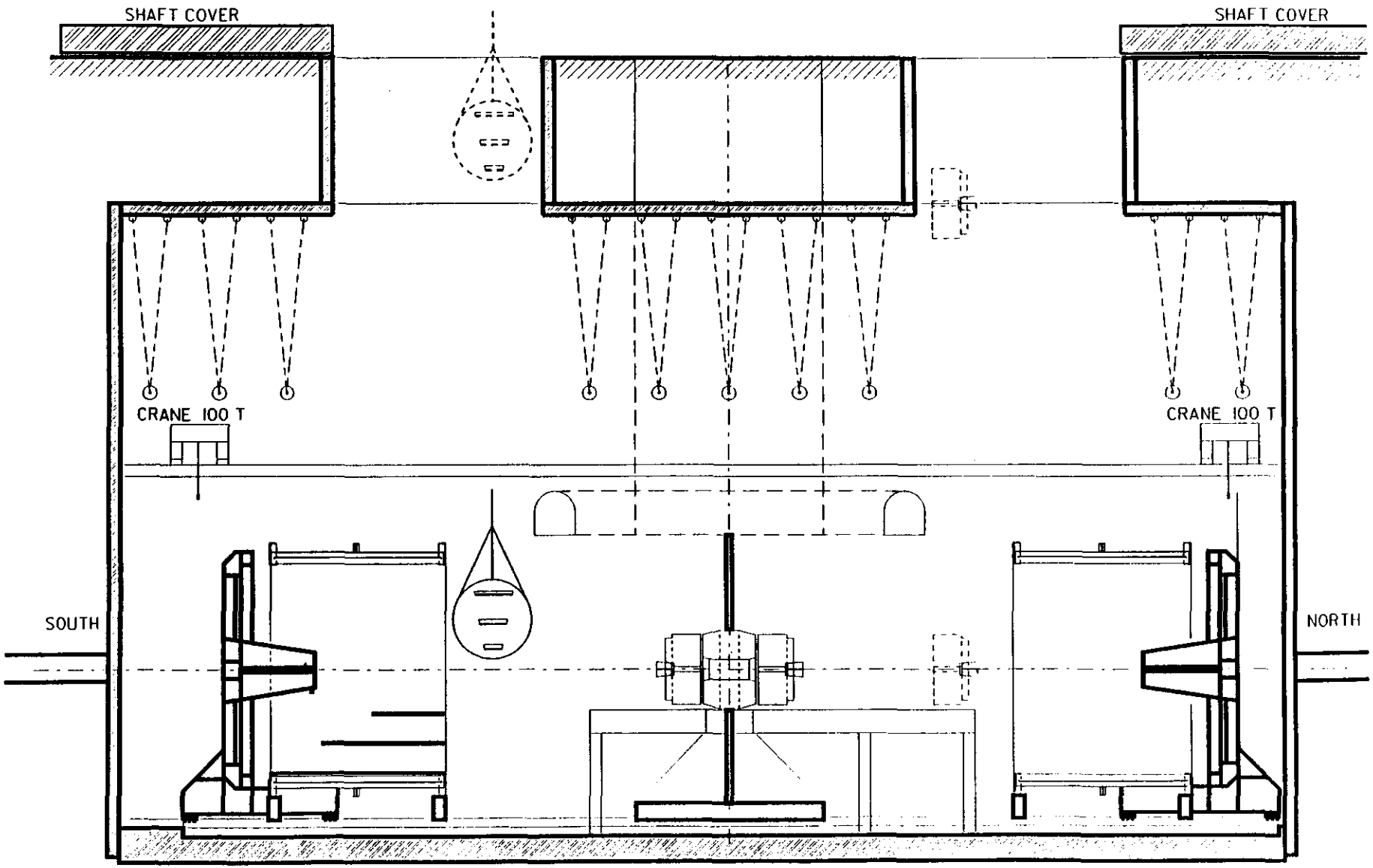

Figure 29

PHASE 13
INSTALL MUON ENDCAP

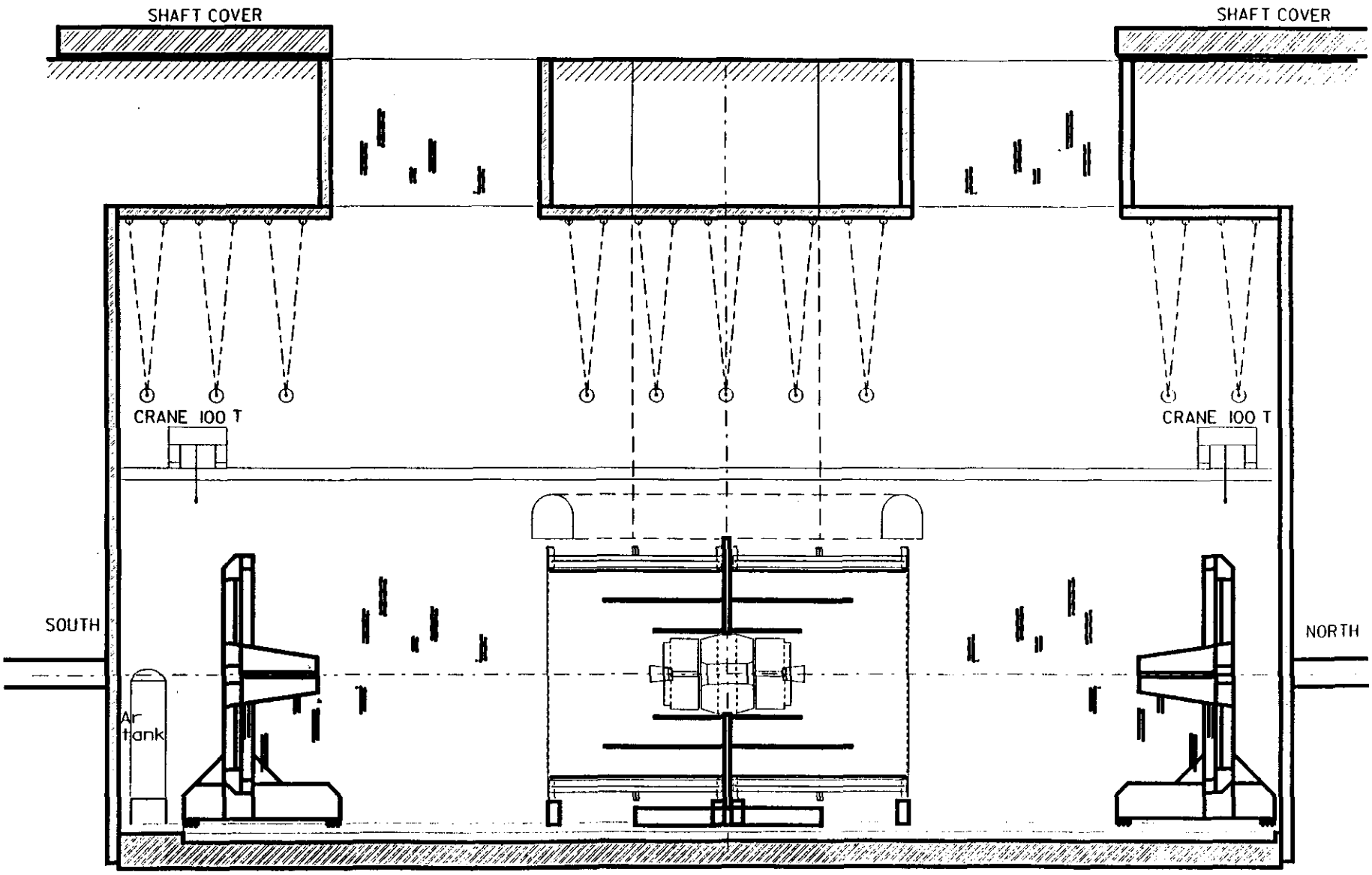

Figure 30

PHASE 14
INSTALL TRACKER - VACUUM PIPE

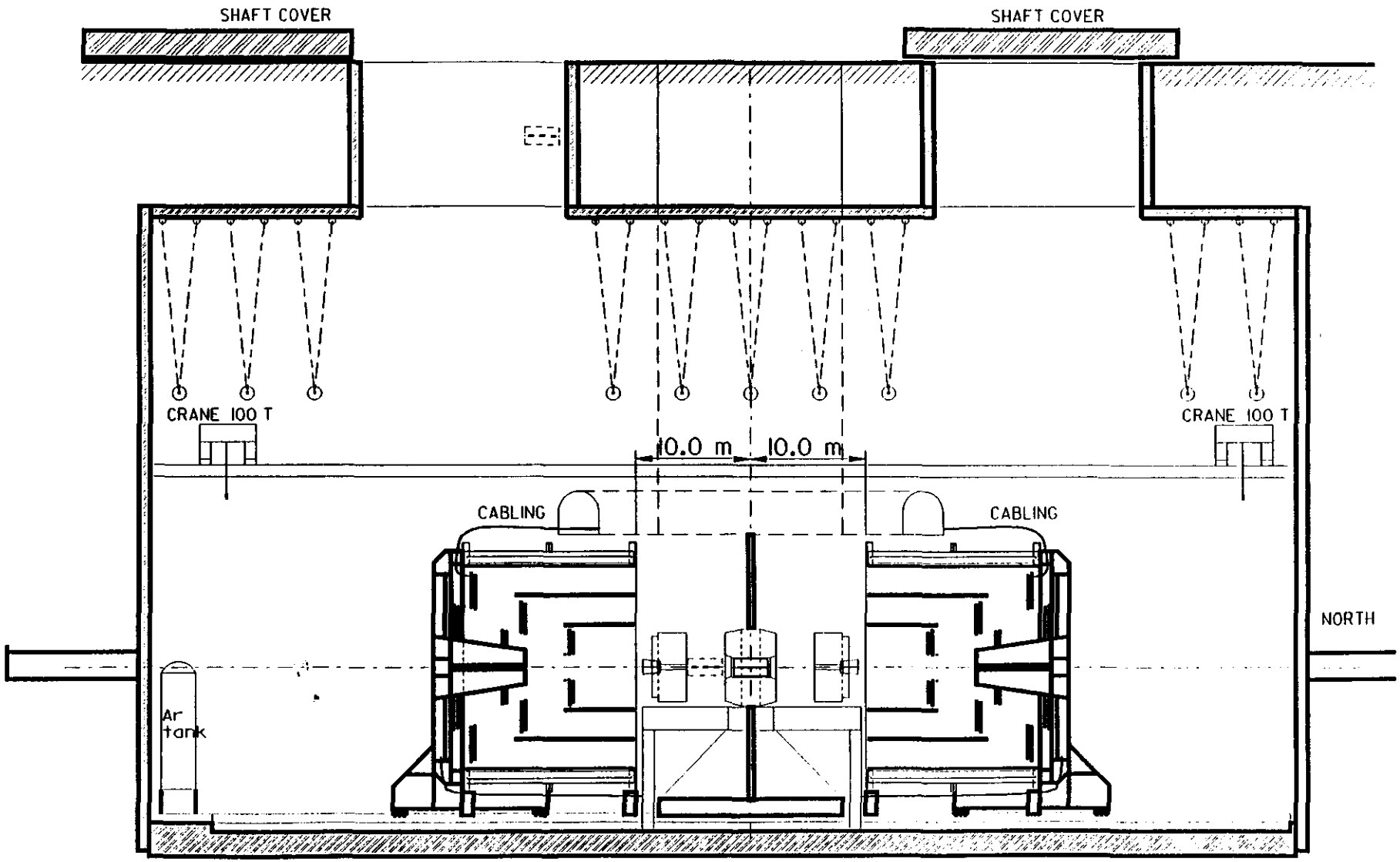

Figure 31

ACCESS LEVEL FIGURE 4

BEAM - FIELD OFF ACCESS BETWEEN COILS - FFS

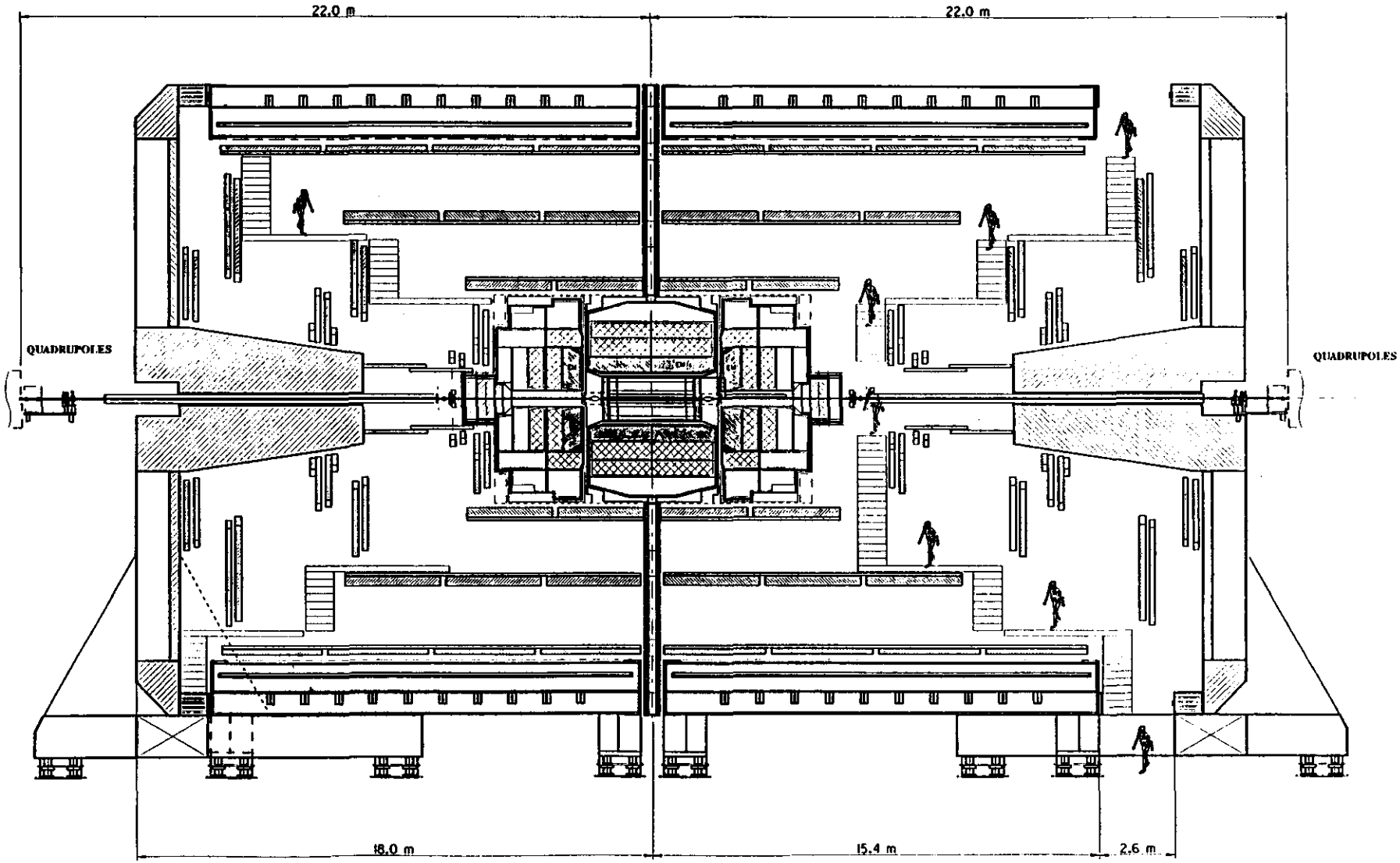

Figure 32

ACCESS LEVEL FIGURE 7
BEAM - FIELD OFF COILS - END CAP CALORIMETER MOVED - SUBSYSTEM DISASSEMBLED

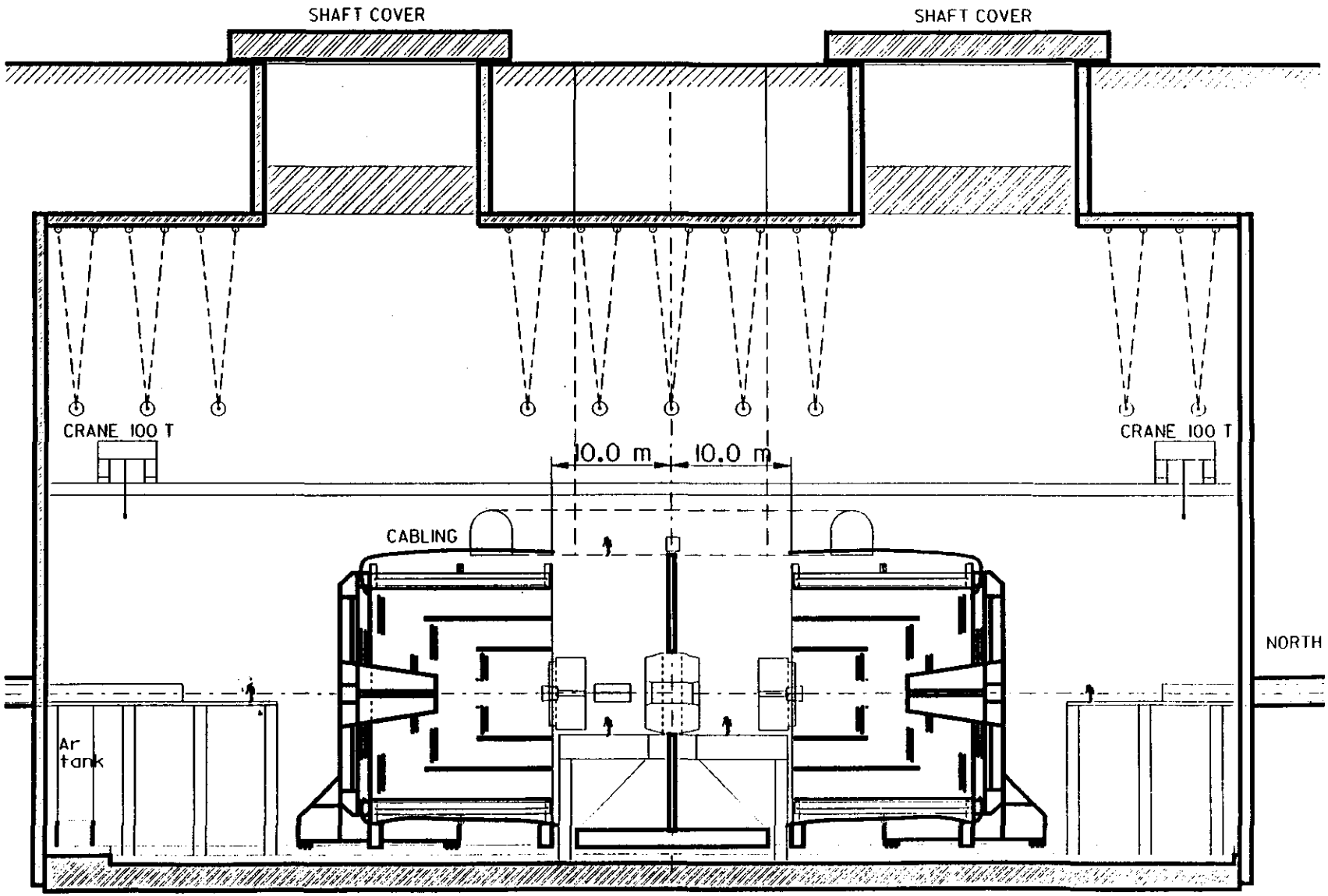

Figure 33

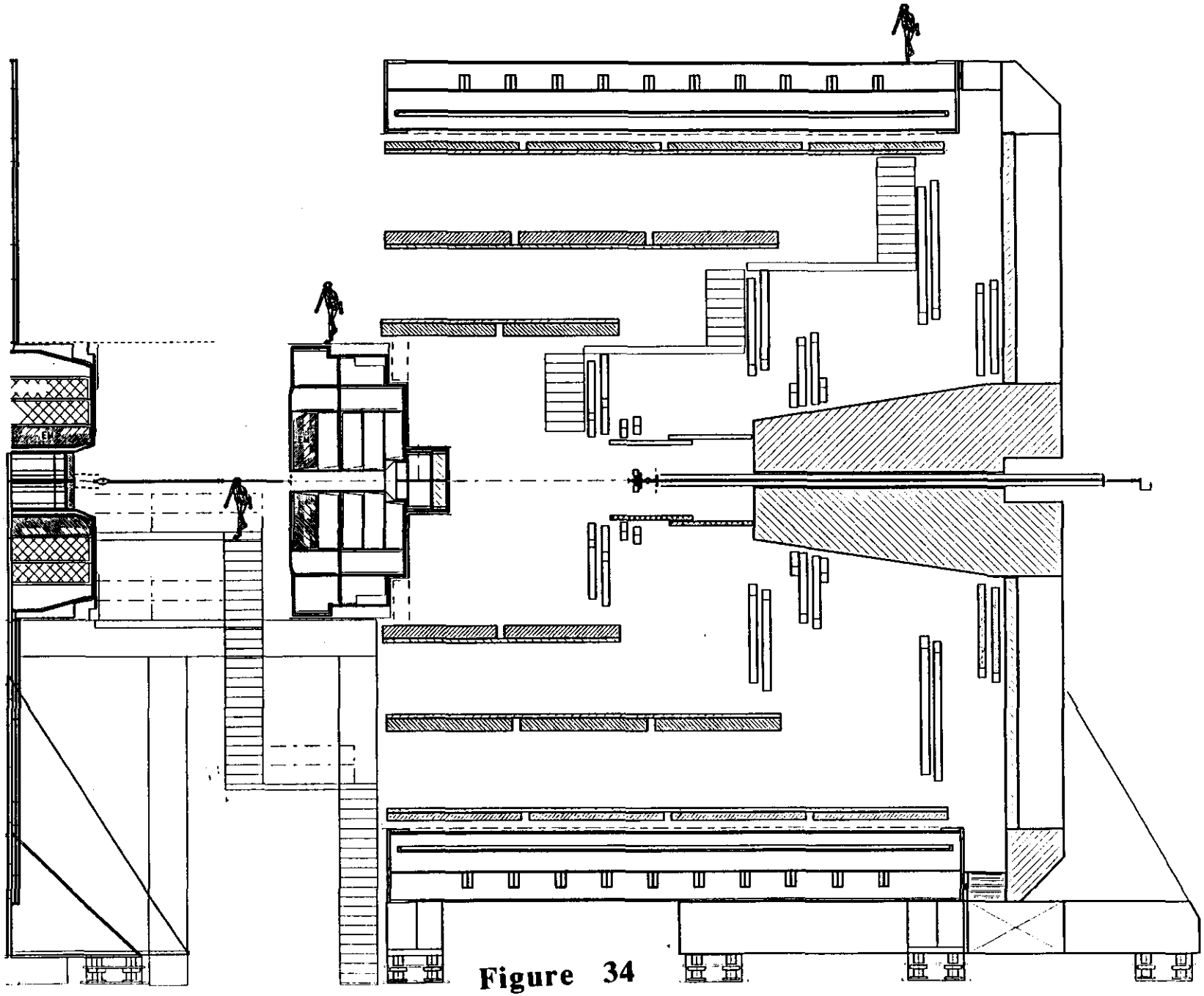

Figure 34